Volume 49
Number 18
21 September 2020
Pages 6517–6792

Chem Soc Rev

Chemical Society Reviews

rsc.li/chem-soc-rev

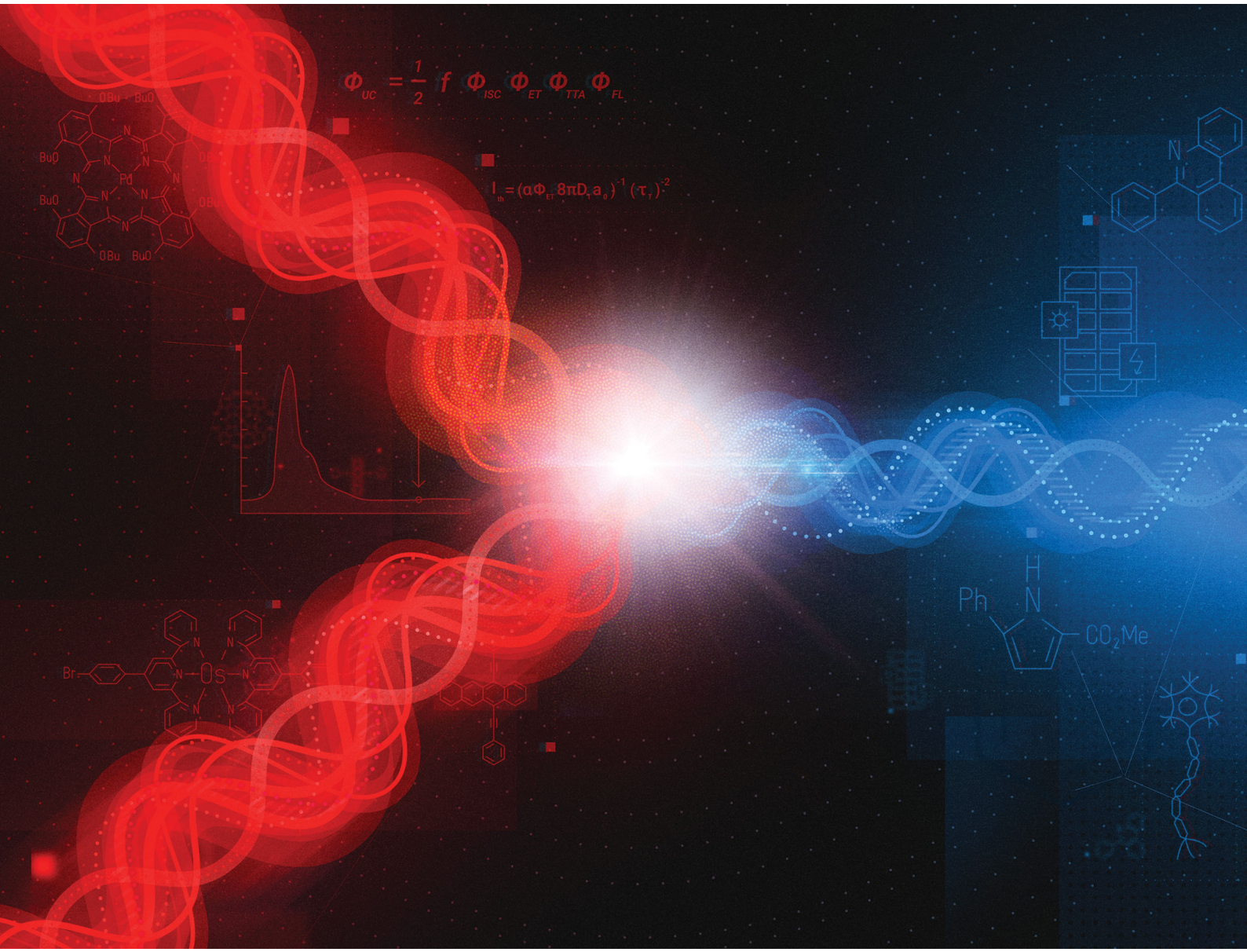

ISSN 0306-0012

ROYAL SOCIETY OF CHEMISTRY

TUTORIAL REVIEW

Pankaj Bharmoria, Kasper Moth-Poulsen *et al.*

Triplet–triplet annihilation based near infrared to visible molecular photon upconversion

Chem Soc Rev

TUTORIAL REVIEW

View Article Online
View Journal | View Issue

Cite this: *Chem. Soc. Rev.*, 2020, **49**, 6529

Triplet–triplet annihilation based near infrared to visible molecular photon upconversion

Pankaj Bharmoria,* Hakan Bildirir and Kasper Moth-Poulsen*

Received 23rd June 2020

DOI: 10.1039/d0cs00257g

rsc.li/chem-soc-rev

Triplet–triplet annihilation based molecular photon upconversion (TTA-UC) is an exciting research area for a broad range of photonic applications due to its tunable spectral range and possible operation at non-coherent solar irradiance. Most of the TTA-UC studies are limited to Visible to Visible (Vis to Vis) energy upconversion. However, for several practical photonic applications, efficient near infrared (NIR) to Vis upconversion is preferred. Examples include, (i) photovoltaics where TTA-UC could lead to utilization of a larger part of the solar spectrum and (ii) in NIR stimulated biological applications where the deep penetration and non-invasive nature of NIR light coupled to TTA-UC offers new opportunities. Although, NIR to Vis TTA-UC is known since 2007, the recent five years have witnessed quite a progress in terms of the development of new chromophores, hybrid systems and fabrication techniques to increase the UC quantum yield at low excitation intensity. With this tutorial review we are reviewing recent progress, identifying existing challenges and discus possible future directions and opportunities.

Key learning points

1. A deeper knowledge of TTA-UC based NIR to Vis photon upconversion.
2. A brief history of TTA-UC with conceptual outline.
3. An increased understanding based on molecular design to make more efficient NIR to Vis TTA-UC systems.
4. An understanding of current state of the art related to NIR to Vis TTA-UC.
5. Challenges and future directions in the development of efficient NIR to Vis TTA-UC Systems.

1. Introduction

Among the emerging artificial light harvesting systems, molecular photon upconversion operating *via* triplet–triplet annihilation (TTA-UC) is investigated for various photonic applications including photovoltaics, bioimaging, photocatalysis, photodynamic therapy, sensing and optogenetics.[1–6] This is due to its operation at tunable wide spectral ranges and its function at low excitation intensities ($\sim$1 mW cm^{-2}) of non-coherent light, corresponding to AM 1.5 solar irradiance intensities and below.[3] TTA-UC is a photochemical phenomenon wherein low energy photons are converted to high energy photons *via* a series of energy transfer processes between chromophores.[7] A typical TTA-UC system is an ensemble of annihilator chromophores doped with triplet sensitizer, wherein after excitation at low energy, the sensitizer transfers its triplet energy to the annihilator, followed by annihilation of two sensitized annihilator triplets, leading to anti-Stokes delayed fluorescence at higher energy (Fig. 1).[1–8] The triplet energy transfer in TTA-UC occurs *via* Dexter energy transfer mechanism (DET) wherein a non-radiative electron exchange occurs between the overlapping wave functions of molecules residing within 10 Å. Although, the triplet sensitized anti-Stokes delayed fluorescent molecular system was first reported by Parker *et al.* in 1962 at −66 °C or −72 °C,[9] actual developments towards realizing its practical utility began in the early 21st century, after the development of heavy metal metal–organic complexes showing long lived triplet population at room temperature. The room temperature anti-Stokes delayed fluorescent molecular system was first reported by Baluschev's research group in 2003, as a sensitizer/annihilator couple film of Pd(II) octaethylporphyrin/polyfluorene showing green to blue TTA-UC.[10] They reported it as a potential solution to increase the efficiency of solar cells beyond Shockley–Queisser limit.[11] This is because TTA-UC can upconvert the transmitted sub-band gap photons to band-gap responsive photons of semiconductor solar cells at the solar irradiance.[1–3] Over the years TTA-UC has grown at various fronts including, UC spectral width (UV to NIR),[12] mechanistic understanding,[13,14] inorganic–organic hybrid systems,[12,15] oxygen sensitivity[8] and applications beyond photovoltaics.[4–6]

Chalmers University of Technology, SE-412 96, Göteborg, Sweden.
E-mail: pankajb@chalmers.se, kasper.moth-poulsen@chalmers.se

Most of TTA-UC systems are limited to visible to visible UC, which have contributed immensely to the conceptual development of the field. However, for several practical photonic applications, NIR to Vis TTA-UC is very appealing. This is because; (1) NIR is weakly absorbed by body tissue and therefore, useful in probing biological systems,[5,6] (2) the broad NIR region is highly desired to increase the efficiency of both semiconductor based and dye sensitized solar cells operating in the visible region[1–3] and (3) deep penetration depth of NIR light can be utilized to generate high energy photons *via* TTA-UC for photocatalysis to realize similar or higher yields than attainable through direct sensitization.[4] Additionally, UC from beyond the band gap of conventional crystalline silicon (c-Si) solar cells (1100 nm), could thwart their Shockley Queisser Limit.[15] Although NIR to Vis UC systems are well known in the form of rare earth metal doped nanocrystals, these materials have challenges in terms of need of high excitation intensity, low UC quantum yield ($<5\%$) and thermal effects.[16] The NIR to Vis TTA-UC systems are emerging as potential solution to these challenges on account of functioning at low excitation intensity. However, the developments in NIR to Vis TTA-UC systems are mainly limited to deoxygenated organic solvents which leads to challenges for device fabrication and is not applicable for *in vivo* applications. This is due to poor solubility of highly hydrophobic NIR to Vis UC dyes in polymers, in addition to triplet quenching by molecular oxygen and poor electronic coupling of sensitizer/annihilator couples due to the spatial difference in orientation of wavefunctions leading to poor triplet energy transfer from sensitizer to annihilator. On grounds of the promising applications offered by NIR light, it is imperative to understand the underlying reasons at the mechanistic level leading to low UC quantum yield of these systems. Therefore, in this tutorial review we are reviewing the developments in NIR to Vis TTA-UC systems in terms of new chromophores, sensitization, energy transfer mechanisms, hybrid systems and fabrication techniques to increase the UC quantum yield at low excitation intensity. Existing challenges and future directions are discussed as guiding path for further research.

Pankaj Bharmoria

Pankaj Bharmoria is an experimental Bio-Photophysical Chemist, with research expertise in photon upconversion, biophotonics, biochemistry and organic/inorganic salt-water chemistry. At present he is working as Marie Skłodowska-Curie Post-Doctoral Researcher with Prof. Kasper Moth-poulsen, at Chalmers University of Technology Sweden. He obtained BSc. (Chemistry, Biology) and MSc. (Chemistry) at Himachal Pradesh University, India and Ph. D (Biophysical Chemistry) under the supervision of Dr Arvind Kumar at AcSIR-Central Salt and Marine Chemical Research Institute, India in 2015. His past Post Doc research career includes, with Professors Mara G. Freire (2016), Sónia P. M. Ventura and João A. P. Coutinho (2019–2020) at CICECO-Aveiro university, Portugal and as JSPS Post Doc fellow with Professors Nobuo Kimizuka and Nobuhiro Yanai at Kyushu University, Japan (2016–2018).

2. Background of molecular TTA-UC

The triplet state is in most molecules an excited quantum state wherein unpaired electrons having same spin can co-exist, leading to a spin angular quantum number of 1 (Fig. 1a). It is a Pauli's spin forbidden state. In the typical TTA-UC scheme,

Hakan Bildirir

Hakan Bildirir received his BSc (Chemistry, 2009) and MSc (Chemistry, 2011) degrees from Istanbul Technical University. After he received PhD title from the Technical University of Berlin (Chemistry, 2015), he worked in Advent Technologies SA-Greece and the Scientific and Technological Research Council of Turkey (TUBITAK). Currently, he holds a position in Chalmers University of Technology, and focuses on synthesis of electron rich organic compounds, porous materials, and their use in the energy related applications.

Kasper Moth-Poulsen

Kasper Moth-Poulsen is a professor in nanomaterials chemistry at Chalmers University of Technology in Gothenburg Sweden. His research interest focus on molecular and nanoparticles synthesis, energy storage, photon up-conversion, and molecular materials. One element of his research is development of devices that demonstrate the function of the materials. He received his MSc (2003) and PhD (2007) degrees in chemistry from University of Copenhagen, Denmark under supervision of professors T. Bjørnholm and J. B. Christensen. In 2009 he joined the groups of R. A. Segalman and K. P. C. Vollhardt at U. C. Berkeley as a Post. Doc. In 2011 he moved to Gothenburg, Sweden to lead his research Group at Chalmers.

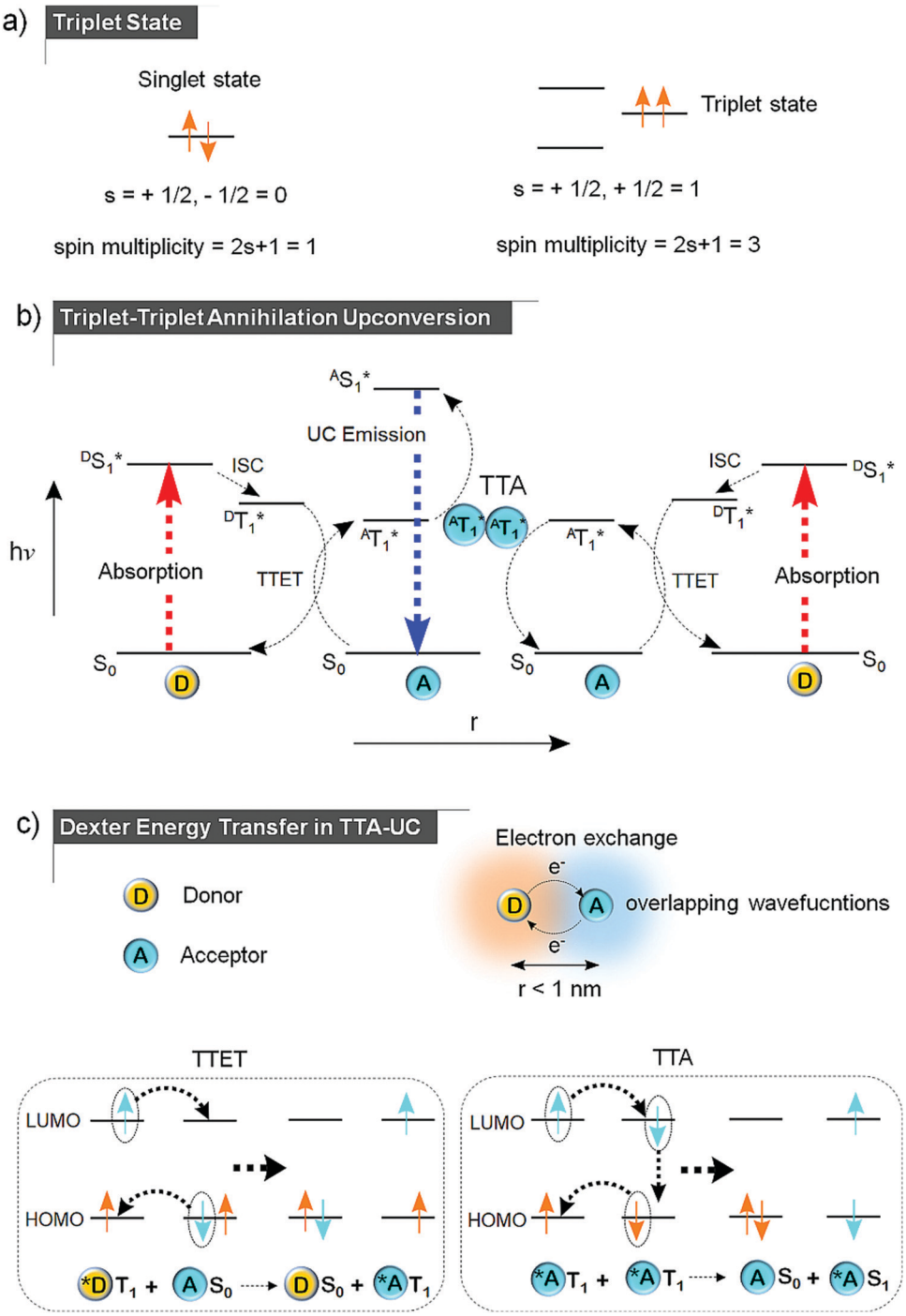

Fig. 1 (a) Difference between singlet and triplet state of a molecule. (b) Jablonski diagram demonstrating the TTA-UC. (c) Demonstration of Dexter energy transfer *via* electron exchange between the overlapping wavefunction's of sensitizer (donor) and annihilator (acceptor) in TTET and between annihilators by TTA.[14]

the singlet excited donor/sensitizer crosses the spin barrier to the triplet state ($^{D}T_1^*$) due to high spin orbit coupling. The sensitizer transfers its triplet energy to the annihilator by triplet–triplet energy transfer (TTET), followed by molecular diffusion or energy migration of sensitized annihilator triplets. When two such sensitized triplets of annihilator collide in the space-time ($^{A}T_1^* \leftrightarrow {}^{A}T_1^*$), the annihilation (TTA) may results in a higher energy singlet excited state ($^{A}S_1^* = 2\cdot{}^{A}T_1^*$) subject to *f* factor which radiates the anti-Stokes delayed fluorescence as depicted in Fig. 1b.[7,8]

The energy difference between the energy of the incoming photon and the emitted photon is called the anti-Stokes shift (ΔE_{UC}). In practice, excitation and emission can occur at different wavelengths, thus creating some ambiguity in the

research field on how to report experimental observations. In this review, we have, for practical reasons calculated the anti-Stokes shift (ΔE_{UC}) as the difference between the excitation wavelength of the sensitizer and wavelength maximum of the upconverted emission of annihilator. This due to the fact that conventionally ΔE_{UC} in the published papers on NIR to Vis TTA-UC has been reported like this. We note that this way of reporting ΔE_{UC} is debated in literature[3] and recommend researchers to onwards follow suggestions as recently put forward by Castellano, Schmidt and Hanson.[17]

TTA-UC is a non-linear optical process, where triplet excited states of several chromophores leads to a higher energy emissive singlet state in the annihilator molecule. Since, the triplet energy transfer among chromophores occurs through electron exchange *via* Dexter energy transfer (DET) mechanism,[14] the chromophores must be present within the distance of 10 Å with respect to each other (Fig. 1c). DET was discovered in 1953 as a radiationless energy transfer between the overlapping wave functions of the donor and acceptor systems in crystalline phosphors. The rate of DET (k_{ET}) between donor and acceptor decreases exponentially with the distance as shown in eqn (1).

$$k_{ET} \propto J_{exp}\left[\frac{-2r}{L}\right] \quad (1)$$

where r is the distance between donor and acceptor, L is the sum of van der Waals radii of donor and acceptor and J is the spectral overlap integral defined by eqn (2).

$$J = \int f_D(\lambda)\varepsilon_A(\lambda)\lambda^4 d\lambda \quad (2)$$

λ is wavelength and ε is molar absorption coefficient. The distance between the donor and acceptor ($r < 1$ nm) is the key for effective overlap of wavefunctions for an electron exchange to occur.

The effective orbital overlap (both distance and molecular orientation) between donor–acceptor systems leads to effective triplet energy transfer resulting in TTA-UC at a certain threshold excitation intensity. The threshold excitation intensity (I_{th}) is defined by eqn (3).

$$I_{th} = (\alpha\Phi_{ET}8\pi D_T a_0)^{-1}(\tau_T)^{-2} \quad (3)$$

where α denotes absorption coefficient at the excitation wavelength, Φ_{ET} denotes sensitizer to annihilator triplet energy transfer efficiency, D_T denotes diffusion constant of annihilator triplets, a_0 denotes the annihilation distance between annihilator triplets and τ_T denotes the lifetime of annihilator triplets. Therefore, for a TTA-UC system to function at around subsolar irradiance, it must have high Φ_{ET} and significant triplet diffusion to achieve low threshold excitation intensity. Experimentally it is calculated from the cross section of slopes in quadratic and linear regimes of the double logarithmic plot of UC emission intensity *vs* incident laser intensity. Besides I_{th}, it is highly desired to have a TTA-UC system, showing high upconversion quantum yield (Φ_{UC}) or upconversion efficiency (Φ_{UC}' or η_{UC}) which is further governed by other photophysical processes. The Φ_{UC} is defined by eqn (4).

$$\Phi_{UC} = \frac{1}{2} f \Phi_{ISC}\Phi_{ET}\Phi_{TTA}\Phi_{FL} \quad (4)$$

$$\eta_{UC} = \Phi_{UC}' = 2 \times \Phi_{UC} \quad (5)$$

where, Φ_{ISC}, Φ_{ET}, Φ_{TTA} and Φ_{FL} denotes quantum yields of sensitizer's intersystem crossing (Φ_{ISC}), sensitizer to annihilator triplet energy transfer (Φ_{ET}), annihilator-annihilator annihilation (Φ_{TTA}) and fluorescence of annihilator (Φ_{FL}). We note that using eqn (4), the value of Φ_{UC} will have a theoretical maximum quantum yield of 50%. In many reports, the authors prefer to report a 100% theoretical maximum which is termed upconversion efficiency (Φ_{UC}') and is denoted by $\Phi_{UC}' = 2 \times \Phi_{UC}$, as shown in eqn (5).[16] Recently it has been recommended to be represented as normalized upconversion efficiency (η_{UC}) by Castellano, Hanson and Schmidt.[17] To allow for direct comparison of reported values of Φ_{UC} and avoid any confusion in this review article, we have recalculated all the values to be mentioned as Φ_{UC} as per eqn (4) except for ref. 12 and 42 whose values are calculated as per eqn (8) shown later.

The parameter f in eqn (4) is referred to as the Spin statistical factor which represents the probability of getting excited singlet state after annihilation of two triplets *via* TTA. The number 1/2, represents the fact that 1 high energy photon is emitted upon absorption of two low energy photons *via* TTA-UC (Fig. 2a). The f is an important parameter in regard to the statistical UC efficiency possible *via* TTA-UC. Statistically

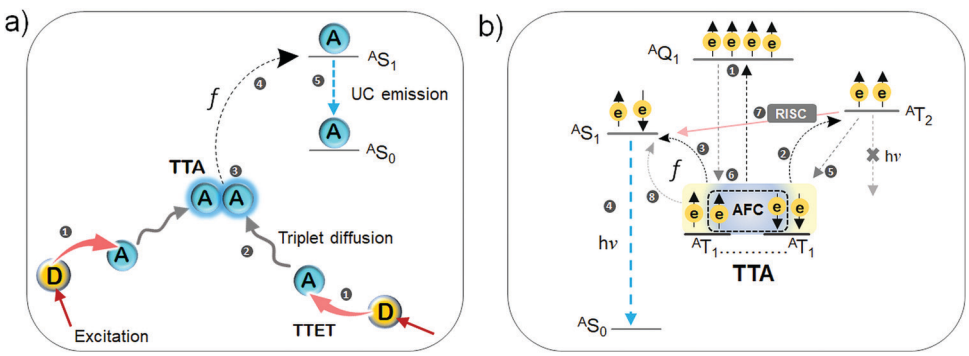

Fig. 2 Artistic presentation of (a) events leading to TTA-UC emission and (b) post TTA events showing the formation of three different energy states of annihilator with different spin multiplicities including singlet ($^AS^1$), triplet ($^AT_2$) and quintet ($^AQ_1$).

TTA between two annihilator triplets in solution can results in three kinds of encounter complexes of which; 1/9 is singlet, 3/9 are triplet and 5/9 are quintet states. The encounter complex formation probabilities are weighed according to their spin multiplicities as 1 : 3 : 5.[18] Out of these, only $^{A}S_1$ decay back to $^{A}S_0$ state to give UC emission *via* singlet channel thus setting 11.1% (1/9) as the maximum statistical limit of *f* factor. This is due to the fact that triplet photons of quintet and triplet encounter complexes are entirely quenched since they cannot relax *via* internal conversion to $^{A}S_1$ state due to the spin restriction. According to the general notion the annihilating triplets undergoes ferromagnetic coupling (FC) during TTA, resulting in encounter complexes of different multiplicity in an energetic order as per Hund's rule (quintet the lowest energy state and singlet the highest), thus discarding the possibility of uphill triplet energy flow into the singlet channel. However, recently this notion has been challenged on grounds of the fact that antiferromagnetic coupling (AFC) among annihilating triplets dominate the ferromagnetic coupling which reverses the spin states energy level order against the Hund's rule, thus making quintet ($^{A}Q_1$) as the highest energy state, followed by triplet ($^{A}T_2$) and singlet ($^{A}S_1$) as shown in Fig. 2b.[18]

This can be understood by eqn (6).

$$E_S = -J\,(S\,(S+1) - 4) \qquad (6)$$

where E_S is energy of the spin state, J is magnetic exchange parameter and S is total angular momentum of annihilating triplets. The parameter J contains all spatial information of the electron wavefunction of two triplets for their interaction through space or through bonds which eventually determines the preferential lowest energy spin state and energetic order. If $J > 0$ then similar spins of two triplets couples *via* ferromagnetic coupling resulting in $^{A}Q_1$ as the lowest energy state, whereas if $J < 0$, then opposite spins of two triplets couples *via* antiferromagnetic coupling leading to $^{A}S_1$ as the lowest energy state (Fig. 2b). The opposite energetic order obtained for FC and AFC can be easily understood by putting the value of $J = +1$ or -1 and $S = 0$, 1 and 2 for singlet, triplet and quintent state in eqn (6). Therefore, the post TTA energetic order obtained *via* antiferromagnetic coupling discards the possibility of complete quenching of the triplet photons of quintet and triplet channels and vouch for their participation in singlet channel (Fig. 2b) to increase the *f* factor beyond 11.1%. The $^{A}T_2$ and $^{A}Q_1$ encounter complexes can relax back to the $^{A}T_1$ state non-radiatively to takes part in TTA reaction again to give $^{A}S_1$. Additionally, the reverse intersystem crossing (RISC) of $^{A}T_2$ to $^{A}S_1$ is also proposed to increase the *f* factor if $^{A}T_2$ and $^{A}S_1$ energy levels are accessible. The *f* factor of 50% (diphenyl anthracene), 33% (rubrene) and even 100% (perylene) are reported now, thus making these annihilators among the popular choices for TTA-UC studies.[18] This is possible by suitable engineering of the energy levels of annihilator *via* chemical modification.

2.1. History of molecular TTA-UC

Historically, the phenomenon of sensitized anti-Stokes delayed fluorescence was first reported by Parker and Hatchard in 1962,[9] for an equimolar mixture of phenanthrene/naphthalene (UV to UV, TTA-UC) with ΔE_{UC} = 0.21–0.43 eV (341 or 362 nm to 322 nm) and proflavine hydrochloride/anthracene (Vis to Vis TTA-UC) with ΔE_{UC} = 0.24 eV (436 nm to 402 nm) in ethanol at -72 ± 3 °C and -66 ± 3 °C with quantum yield of ~1% and 0.1% respectively (Fig. 3).

Further developments in TTA-UC systems had to wait until the advent of 21st century. One reason could perhaps be the few available molecules showing long lived triplet states at room temperature. However, the development in heavy metal–organic

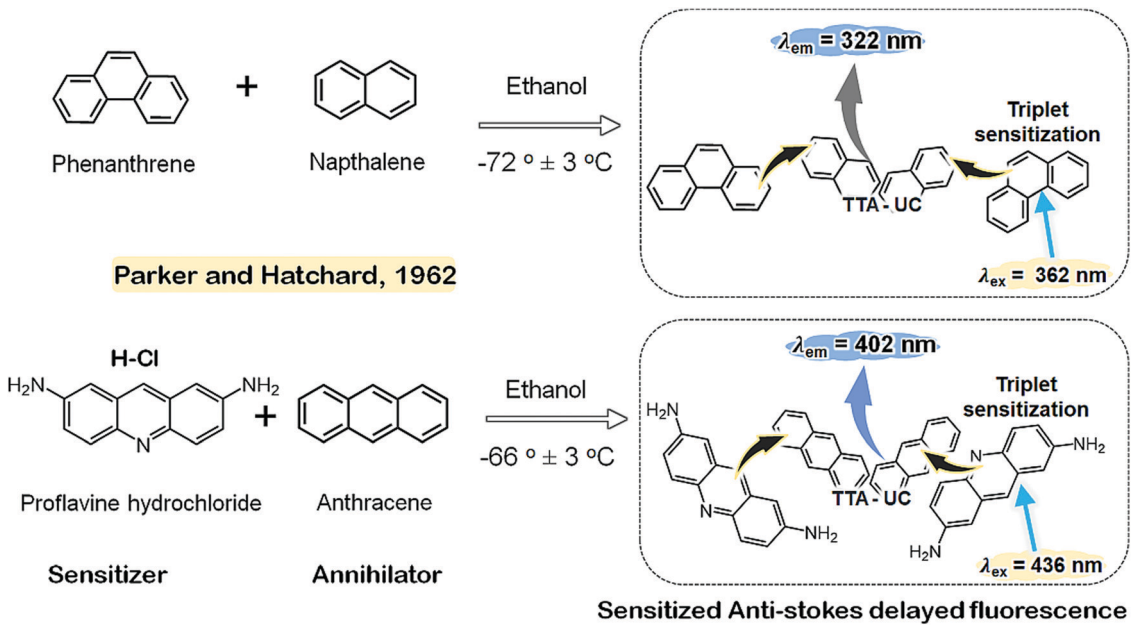

Fig. 3 Illustration of Parker and Hatchard's experiment of sensitized delayed anti-Stokes fluorescence in phenanthrene/naphthalene (362 nm to 322 nm) and proflavine hydrochloride/anthracene (436 nm to 402 nm) couples in ethanol.[9]

complexes in last phase of 20th century, of which many show long lived triplet states at room temperature eventually created opportunities for TTA-UC that emerged as a vibrant research field. The first demonstration of room temperature sensitized delayed TTA-UC (Green to blue) was published by Baluschev and co-workers, as an approach to increase the efficiency of solar cells.[10] Previously known photon upconverting systems like inorganic materials, nanoparticles and organic two photon absorption (TPA) systems had challenges with the need of high excitation intensities paired with lower UC efficiencies. The poly(9,9-bis(2-ethyl-hexyl)fluorene) (PF_2/6) solid film, doped with Pd(II) octaethylporphyrin showed an energy upconversion with $\Delta E_{UC} \sim 0.6$ eV (532 nm to 424 nm), at an excitation intensity of 13.5 kW cm^{-2}.[10] This excitation intensity was six orders of magnitude less (19.5 GW cm^{-2}) than previously reported comparable systems based on TPA.

Baluschev's research group realized the potential of TTA-UC in photovoltaics when Pd(II) octaethylporphyrin (PdOEP)/diphenylanthracene (DPA) couple showed green to blue UC emission at low excitation intensity (10 W cm^{-2}) using non-coherent green sunlight (Fig. 4).[11] The demonstration of the use of low intensity sunlight served as an illustration that future solar cells, with integrated TTA-UC systems could function at AM 1.5 solar irradiance.

These early papers spurred an increasing interest in the research community that eventually lead to new conceptual developments like molecular engineering for molecular assembly/co-assembly,[14,19] TTA-UC liquid/liquid crystal/crystal/metal organic frameworks,[20–23] TTA-UC gels,[6,19] oxygen protection strategies,[8] inorganic–organic hybrid TTA-UC,[12,15] triplet energy transfer mechanisms (triplet energy migration, entropy driven triplet energy transfer, direct S_0 to T_1 energy transfer and solvent effects),[7,14] new sensitizers (semiconductor quantum dots, boron-dipyrromethene (BODIPY) radicals, thiosquaraines, direct S_0-to-T_1 absorbing osmium complexes, TADF and perovskites nanocrystals,),[13] annihilators (supramolecular, transmitters, self-assembling, and ionic),[7,19] triplet loss channels *etc.* Moreover, the applications of TTA-UC systems also evolved into areas of photocatalysis, bioimaging, sensing, theranostics and opto-genetics. However, the practical feasibility of these applications beyond lab scale demonstration will require, in most cases, TTA-UC to expand beyond Vis to Vis UC to NIR to Vis UC, on grounds of advantages offered by NIR light discussed in the introduction section. Various developments in NIR to Vis TTA-UC in terms of molecular design, ΔE_{UC}, Φ_{UC} and I_{th} are summarized in Table 1.

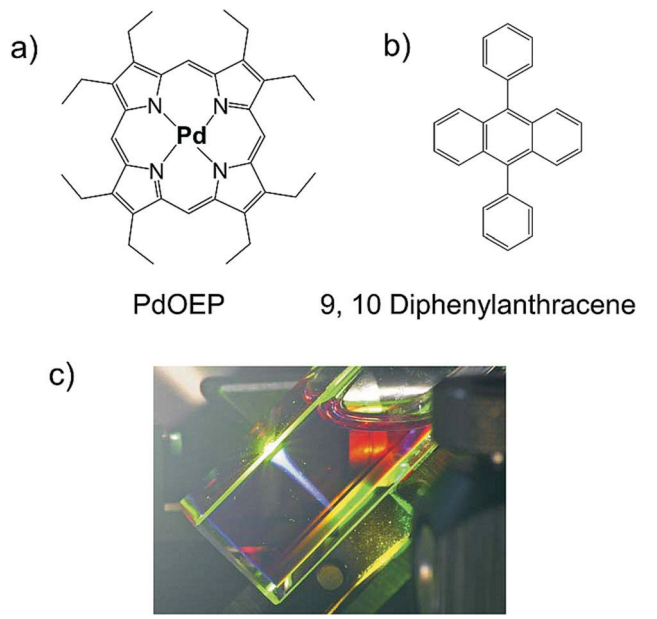

Fig. 4 (a) and (b) Molecular structures of (a) PdOEP (sensitizer), and (b) 9,10-diphenylanthracene (annihilator). (c) A CCD-camera image of the up-converted fluorescence inside the 1 cm cuvette, excited with the green part of the sun spectrum, no filters were used. Reproduced with permission from ref. 11, Copyright, 2006 The American Physical Society.

2.2. Background of NIR to Vis Molecular TTA-UC

Baluschev and co-workers were the first to report NIR to Vis TTA-UC, for *meso*-tetraphenyl-octamethoxide-tetranaphtho[2,3]-porphyrin palladium ($PdPh_4OMe_8TNP$)/Bis(phenyltetracene) couple in deaerated toluene solution in 2007 (Fig. 5).[24] They reported $\Delta E_{UC} \sim 0.71$ eV (695 nm to 497 nm) with $\Phi_{UC} = 4\%$ (calculated using actinometry method). Interestingly, they excited the sample with non-coherent NIR light, at an excitation intensity of 1 W cm^{-2} and a spectral width of $\Delta\lambda \sim 20$ nm. Moreover, it was for the first time that triplet energy state of as low as 1.3 eV was harvested by photon upconversion, giving strong motivation for further exploration.[24]

Subsequently, they also reported the harvesting of non-coherent NIR light by changing the annihilator to 9,10-bis(phenylethynyl)-naphthacene (BPEN) with same sensitizer, $PdPh_4OMe_8TNP$ in deaerated toluene solution (Fig. 6a–c).[25] Interestingly, the ΔE_{UC} = 0.39 eV (695 to 570 nm) was observed at a low excitation intensity of 150 mW cm^{-2}, with $\Phi_{UC} = 3.2\%$. In the same paper, they also demonstrated a new concept for step wise TTA-UC to achieve 700 nm to 400 nm UC (ΔE_{UC} = 1.33 eV) by selecting a series of sensitizer–annihilator couples and exciting at different wavelengths using non-coherent light (Fig. 6d).[25]

Ideally, such a large ΔE_{UC} should be achieved with single excitation of non-coherent NIR light, followed by subsequent upconverted emission-absorption cycles of respective wavelengths in a linearly fabricated sensitizer–annihilator couple systems, ranging from NIR to near UV region. Although, it could not be realized till date due to the low UC quantum yield of NIR to Vis TTA-UC systems. However, recently a large ΔE_{UC} = 1.28 (724 nm to 415 nm) has been achieved in a single sensitizer/annihilator couple by Kimizuka and Yanai's research groups discussed later.

Castellano's research group were the first to cross the 700 nm excitation energy barrier by introducing a new sensitizer/annihilator couple based on Pd(II) Phthalocyanine ($PdPc(OBu)_8$/rubrene) (Fig. 7) They achieved ΔE_{UC} = 0.5 eV (725 nm to 560 nm) in deaerated toluene solution.[26] The UC emission intensity showed quadratic dependence on the excitation intensity indicating non-linear optical phenomenon.

However, rubrene was shown to be prone to endoperoxidation upon interaction with singlet oxygen generated by interaction of

Table 1 NIR to Vis molecular TTA-UC systems along with their UC performances

Sensitizer/annihilator couple	Solvent/matrix	UC range (nm)	ΔE_{UC} (eV)	I_{th} (W cm^{-2})	Φ_{UC} (%)
($PdPh_4OMe_8TNP$)/bis(phenyltetracene)[24]	Toluene	695 to 497	0.71	—	4.0
($PdPh_4OMe_8TNP$)/BPEN[25]	Toluene	695 to 570	0.39	—	3.2
$PdPc(OBu)_8$/rubrene[26]	Toluene	725 to 560	0.5	—	—
PdTAP/rubrene[27]	Toluene	785 to 568	0.6	—	1.21
Pyr_1RuPZn_2/PDI or tetracene[28]	MTHF	780 to 541	0.7	—	0.375
		780 to 505	0.86	—	—
PtTPTNP/PDI[30]	Toluene	690 to 580	0.34	—	3.0
PtTPTNP/rubrene[30]		690 to 560	0.42	—	3.3
Texaphyrin/rubrene[32]	DCM	750 to 560	0.56	—	0.77
PtNac/TDI[33]	DCB	856 to 690	0.34	—	0.0089
PdNac/TDI[33]		856 to 690		30	0.067
PbSe/rubrene[34]	Toluene	980 to 561	0.94	—	—
		808 to 561	0.67	—	0.005
PbS/CPT (T)/rubrene[35]	Toluene	808 to 561	0.67	—	0.85
PbSe/CPT (T)/rubrene[35]		808 to 561	0.67	—	1.05
PbS-CdS/5-CT (T)/rubrene[36]	Toluene	808 to 561	0.67	0.0032	4.2
PbS/TES-ADT[15]	Toluene	1064 to 610	0.86	43	0.047
PbS-$^1\Delta_gO_2$ (M)/V79[37]	Toluene*	1140 to 700	0.68	—	—
PbS-TTCA/V79[37]	Toluene	808 to 700	0.24	—	0.015
Osmium complex/rubrene[38]	DCM	938 to 570	0.86	—	0.0024
	PVA*	938 to 580	0.83	10	0.215
$Os(bptpy)_2^{2+}$/TTBP[39]	DMF	724 to 462	0.97	0.32	1.35
	PVA*	724 to 489	0.83	—	0.055
$Os(peptpy)_2^{2+}$/TTBP[6]	DMF	724 to 484	0.85	0.66	2.95
	Hydrogel*	724 to 490	0.83	13	< 0.05
$Os(tpy)_2^{2+}$/$(i\text{-}Pr_2SiH)_2An$[40]	THF	724 to 415	1.28	9.6	5.5
	Crystal	724 to 433	1.15	—	0.01
Yb-L/rubrene[41]	D-THF	980 to 559	0.95	—	< 0.5
PdPc/rubrene[18]	Toluene	730 to 560	0.52	1.9	5.6
PtPc/rubrene[18]	Toluene	730 to 560	0.52	11	4.9
PdPc/*t*-but-rubrene[18]	Toluene	730 to 562	0.51	3.6	1.3
PbS–rubrene–DBP (E)[42]	Crystal	808 to 612	0.49	0.012	0.6†
PbS-rubrene–DBP (E)[12]	Crystal	808 to 610	0.5	—	3.5†
PbS/T-MOF[22]	MOF	785 to 550	0.68	13	—
$Os(tpyCOOH)_2^{2+}$/CPAEBA[23]	MOF film*	724 to 540	0.58	10	0.006
PdTPTAP/rubrene[43]	Solid	785 to 570	0.6	0.116	0.5
PdPc-TBR-BDP (E)[44]	PST-film*	730 to 610	0.33	2.4	0.3
$Os(bptpy)_2^{2+}$/G-cyclophane[20]	Crystal	730 to 546	0.57	0.24	0.1
$Os(bptpy)_2^{2+}$/Y-cyclophane[20]	Liq-crystal	730 to 573	0.47	2.5	0.01

T = transmitter and E = emitter, M = Mediator, DCB = dichlorobenzene, DCM = dichloromethane, MTHF = methyl tetrahydrofuran, PVA = polyvinylalcohol, DMF = dimethylformamide, MOF = metal organic framework, PST = polystyrene, * = aereated environment. ΔE_{UC} = emission maxima of upconverted annihilator – excitation wavelength of sensitizer. I_{th} = Crossing point of slopes in quadratic and linear regime of UC emission intensity *vs* excitation intensity plot. Φ_{UC} (50% theoretical maximum). † = calculated using modified eqn (8) where they divided the UC quantum yield with fluorescence quantum yield of annihilator with the laser excitation.

triplet states with molecular oxygen. Castellano's research group therefore demonstrated solid state TTA-UC by blending the molecular UC system in an ethyleneoxide/epichlorohydrin copolymer thin film. The copolymer blended film showed bright yellow UC emission upon continuous excitation, which disappeared with time due to oxygen diffusion into the copolymer film and consequent degradation of rubrene.[26]

NIR excitation at 785 nm was achieved in the same year by Baluschev's research group *via* a new extended π-conjugated Palladium(II) tetraanthraporphyrin (PdTAP) sensitizer showing Q-band absorption at around 800 nm (Fig. 8).[27]

The PdTAP/rubrene couple in deaerated toluene showed $\Delta E_{UC} \sim 0.6$ eV, upon 785 nm laser excitation with Φ_{UC} = 1.21%.[27] Moreover, they observed sublinear dependence of the UC emission intensity on the laser excitation intensity which was unlike the classical TTA of organic crystals where this behavior is linear. The explanation brought forward for this behaviour was that in sensitized TTA, the annihilator triplets are generated due to triplet sensitization by the sensitizer at low excitation wavelength rather than high energy excitation in classical TTA of organic crystals. They called it "energetically conjoined TTA", which show TTA-UC at excitation intensity six orders of magnitude lower than the classical TTA. This could be due to the high emitter triplet population available for annihilation, supplemented by the sensitizer with high ISC coefficient. They also reported stable TTA-UC for more than 60 days when the sample is prepared at <0.1 ppm of O_2, thus highlighting the severity of rubrene for practical TTA-UC applications.[27]

Castellano's research group then in 2010, introduced a photostable alternative to rubrene in the form of perylenediimide (PDI) along with a new conjugated supramolecular sensitizer, ruthenium(II) [15-(4′-ethynyl-(2,2′;6′,2″-terpyridinyl))-bis[(5,5′,-10,20-di(2′,6′-bis(3,3-dimethylbutoxy)phenyl)porphinato)-zinc(II)]ethyne][4′-pyrrolidin-1-yl-2,2′;6′,2″-terpyridine]bis(hexafluorophosphate) (Pyr_1RuPZn_2), which showed stable energy upconversion with ΔE_{UC} = 0.7 eV (780 nm to 541 nm) upon

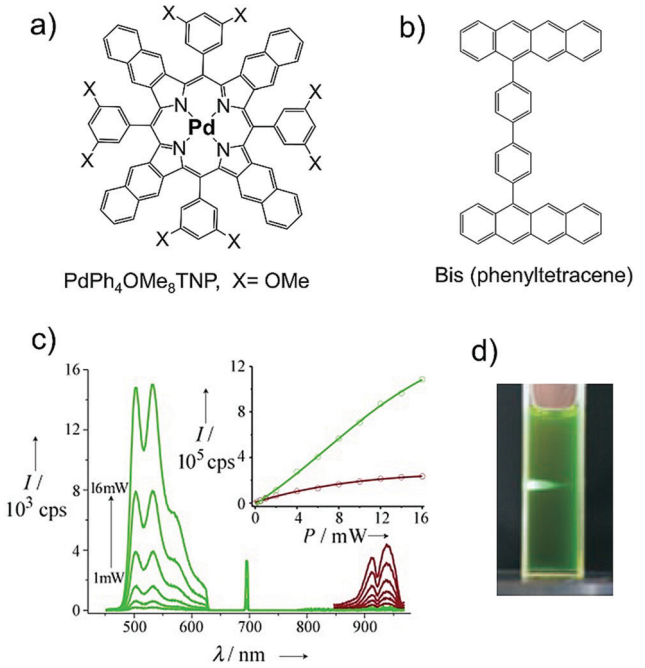

Fig. 5 (a) and (b) Molecular structures of (a) $PdPh_4OMe_8TNP$ (sensitizer), and (b) bis(phenylanthracene) (annihilator). (c) Comparison of the phosphorescence of a toluene solution containing only the sensitizer (1×10^{-4} M; red lines) and the fluorescence of a blended toluene solution of 2×10^{-3} M annihilator and 1×10^{-4} M sensitizer (green lines) at different excitation intensities. Inset: Integral phosphorescence (red circles) and integral fluorescence (green circles) as a function of the excitation intensity. (d) A charge-coupled device (CCD) camera image of the up-converted fluorescence inside the 1 cm-wide cuvette; the fluorescence was excited with the near-infrared part of the solar spectrum, and no filters were used. Reproduced with permission from ref. 24, Copyright, 2007 Wiley-VCH Verlag GmbH & Co. KGaA, Weinheim.

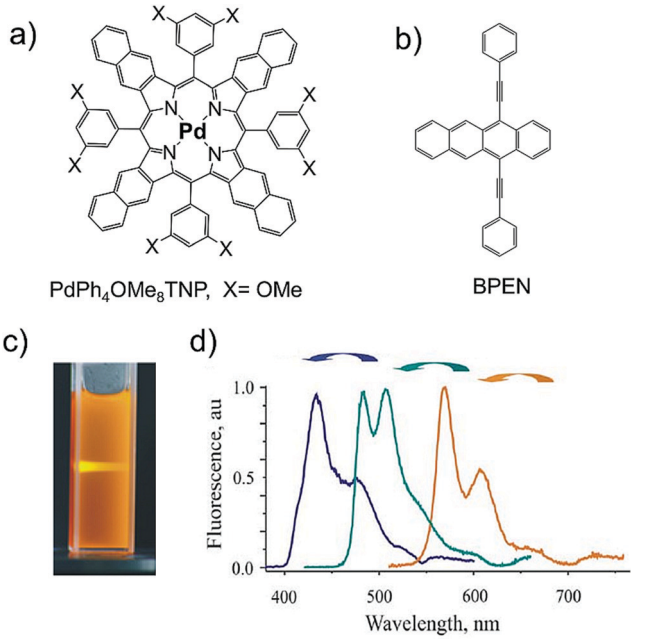

Fig. 6 (a) and (b) Molecular structures of (a) $PdPh_4OMe_8TNP$ (sensitizer), and (b) BPEN (annihilator), (c) a CCD-camera image of the up-converted fluorescence inside a 1 cm cuvette, for BPEN/PdPh4OMe8TNP, excited with the corresponding part of the Sun's spectrum, 1 W cm^{-2}. For the CCD-images no blocking filters were used. (d) Up-conversion fluorescence spectrum of DPA/PdOEP (navy blue line), BPEA/$PdPh_4TBP$ (dark cyan line) and BPEN/$PdPh_4OMe_8TNP$ (orange line) in solution, excitation intensity 1 W cm^{-2}, excited by a portion of solar spectrum (d). Reproduced with permission from ref. 25. Copyright, 2008 IOP Publishing Ltd and Deutsche Physikalische Gesellschaft.

780 nm laser excitation in deoxygenated 2-methyltetrahydrofuran solution (Fig. 9).[28]

Upon combining with another annihilator, tetracene the Pyr_1RuPZn_2/tetracene couple showed energy upconversion anti-Stokes shift of ΔE_{UC} = 0.86 eV (780 nm to 505 nm) upon excitation in deoxygenated 2-methyltetrahydrofuran solution. However, the photostable PDI showed low Φ_{UC} = 0.375%[28] compared to rubrene as an annihilator.[27] They suggested two major factors for low Φ_{UC}; (i) low triplet energy transfer from Pyr_1RuPZn_2 to PDI due to poor electronic coupling caused by the large spatial triplet wavefunction of Pyr_1RuPZn_2 and (ii) low yield of $^1S_1$ after ^{3}PDI–^{3}PDI* TTA annihilation reaction leading to low *f* factor.

Against the conventional approaches Schmidt's research group introduced the positive aspect of molecular oxygen in TTA-UC wherein singlet oxygen generated upon photoexcitation of sensitizer molecule acted as energy mediator to annihilator rather than quencher for NIR to Vis spectrum upconversion (Fig. 10).[29] They called it singlet oxygen mediated upconversion (SOMUC).

In a proof of concept demonstration, the sensitizer/annihilator couple of IR820/V79 showed delayed fluorescence emission only in the presence of O_2 upon excitation at 830 nm. No UC emission was observed in the absence of oxygen thus indicating a SOMUC mechanism (Fig. 10d and e).

Castellano's research group introduced another perylenediimide (PDI) derivative possessing longer alkyl chains as a photostable alternative to rubrene along with a new sensitizer, Platinum tetraphenyltetranaphtho[2,3]porphyrin (PtTPTNP). The PtTPTNP/(PDI), couple which showed efficient UC emission with ΔE_{UC} = 0.34 eV (690 nm to 580 nm) upon 690 nm laser excitation (Fig. 11).[30] Alternatively, the PtTPTNP/rubrene couple showed $\Delta E_{UC} \sim$ 0.42 eV (690 nm to 560 nm).

They reported that PtTPTNP/PDI system showed similar Φ_{UC} = 3 ± 0.25% to that of PtTPTNP/rubrene system (Φ_{UC} = 3.3 ± 0.2%) in deoxygenated toluene solution, therefore, proposed as a photostable alternative to rubrene.

In the meantime, Zhao's research group reported a new triplet sensitizer, Pt(II) bisacetylide complex (Pt-NDI) to harvest triplet energy in the NIR region (1.58 eV = 784 nm).[31] Later they also developed a series of BODIPY dyes as heavy metal free triplet sensitizers[13] to harvest the NIR triplets for Vis to Vis TTA-UC for photodynamic therapy.

In 2014, Castellano's research group introduced an alternative sensitizer, texaphyrin (TXP), containing Cd(II) as metal center. The TXP/rubrene couple in deoxygenated dichloromethane solution showed TTA-UC with ΔE_{UC} = 0.56 eV (750 nm to 560 nm), and Φ_{UC} = 0.77 ± 0.02% (Fig. 12).[32]

Kimizuka and Yanai's research groups introduced metallonaphthalocyanines (PtNac/PdNac) as new triplet sensitizers to

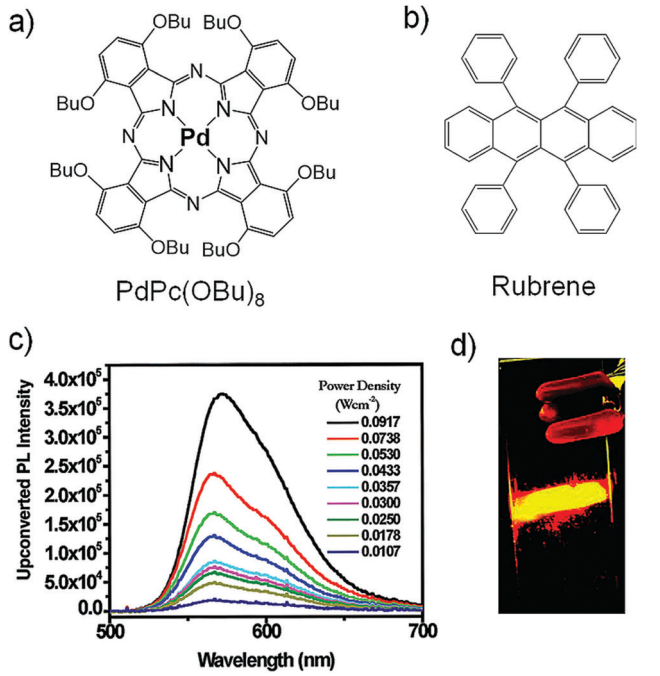

Fig. 7 (a) and (b) Molecular structures of (a) Pd(II) phthalocyanine (sensitizer) and (b) rubrene (annihilator). (c) Delayed fluorescence spectrum of a toluene solution containing 1.61×10^{-5} M $PdPc(OBu)_8$ and 5.86×10^{-4} M rubrene measured 8 μs after a 725 nm, 2 mJ per pulse at 10 Hz. (d) Digital photograph of upconverted fluorescence observed in the P(EO/EP) material containing 2.0×10^{-5} M $PdPc(OBu)_8$ and 6.0×10^{-4} M rubrene taken during an incident 725 nm, 2 mJ laser pulse. Reproduced with permission from ref. 26. Copyright 2008, American Chemical Society.

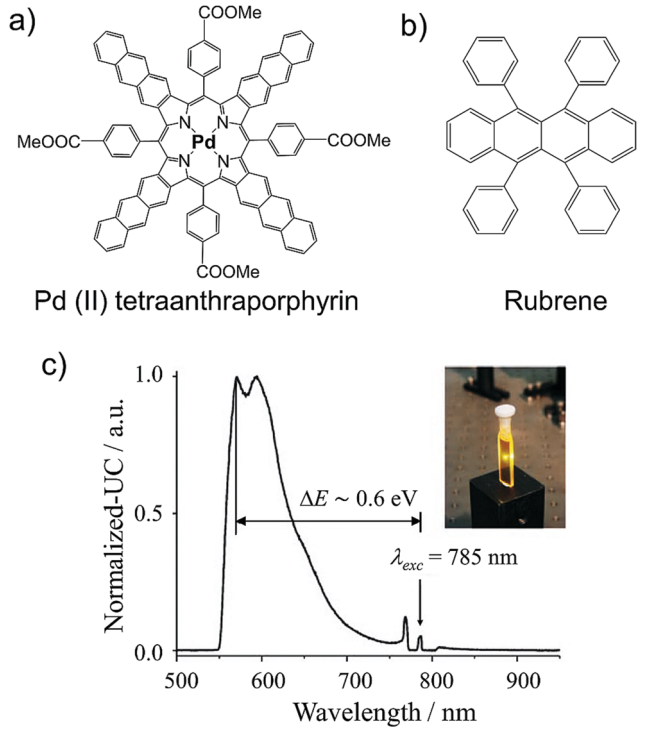

Fig. 8 (a) and (b) Molecular structures of, (a) Pd(II) tetraanthraporphyrin (sensitizer), and (b) rubrene (annihilator). (c) Normalized fluorescence of rubrene excited in upconversion regime at room temperature in toluene, excitation intensity 250 mW cm^{-2} (laser power 10 mW, collimated beam with diameter d = 2 mm), λ = 785 nm. Inset: A CCD-camera image of the up-converted fluorescence inside the 1 mm cuvette, no optical filters were used. Reproduced with permission from ref. 27. Copyright 2008, Wiley-VCH Verlag GmbH & Co. KGaA, Weinheim.

harvest NIR light beyond 850 nm using a new photostable annihilator, terrylenediimide derivative (TDI) as shown in Fig. 13a–c.[33] Both PtNaC/TDI and PdNaC/TDI couples showed photostable NIR to red energy upconversion with $\Delta E_{UC} \sim 0.34$ eV (856 nm to 690 nm) in deaerated dichlorobenzene solution, with Φ_{UC} = 0.0089% and 0.067% respectively. They also reported threshold excitation intensity (I_{th}) from crossing points of slopes in quadratic and linear region for PdNaC/TDI couple to be 30 W cm^{-2}.

Until, 2015, the scarce research on NIR to Vis TTA-UC was largely limited to demonstration experiments in deoxygenated organic solvents with metal porphyrins and phthalocyanines as sensitizers with various annihilators.[24–30,32,33] However, recent five years (2015–2020) have witnessed a lot of activity in NIR to Vis TTA-UC in terms of new molecular designs, inorganic–organic hybrid systems and fabrication techniques to move towards realization of practical applications. Therefore, in the coming section we will discuss breakthroughs in NIR to Vis TTA-UC, in terms of new sensitizers and annihilators and new conceptual design.

3. New directions in NIR to Vis molecular TTA-UC

3.1. Inorganic–organic hybrid NIR to Vis molecular TTA-UC

Inorganic nanocrystals (NCs) due to their tunable band gap can cover the broad absorption range of solar spectrum including the NIR region. This is due to the quantum confinement effect (QCE). Moreover, the QCE allows tuning of the fine electronic structure of NCs. The exchange interactions between the singlet and triplet states of NCs at the band edge is around 1–25 meV and high spin–orbit coupling mixes the electronic orbitals and spin state in such a way that the lowest exciton possesses both singlet and triplet character. Therefore, unlike porphyrins the exciton after direct excitation can sensitize the annihilator if present within the Dexter distance, which takes energy loss during ISC out of equation (Fig. 1b).[12] Moreover, due to the mixed spin state of NCs, the spin state is conserved and energy transfer to the annihilator is spin allowed. The fine electronic structure of NCs at the band edge, allows many electronic states to transfer their triplet energy to sensitize the dark triplets of suitable annihilators.

Vouching on such properties of NCs, in 2015 Tang and Bardeen's research groups introduced inorganic–organic hybrid NIR to Vis TTA-UC, by coupling semiconductor nanocrystal, PbSe as NIR sensitizer and rubrene as molecular annihilator. The degassed toluene solution of PbSe/rubrene showed record energy upconversion anti-Stokes shift with $\Delta E_{UC} \sim 0.94$ eV (980 nm to 561 nm) upon 980 nm laser excitation (Fig. 14a and b).[34] Additionally they also excited the sensitizer at 808 nm leading to the ΔE_{UC} = 0.67 eV (808 nm to 561 nm). Although, it was a

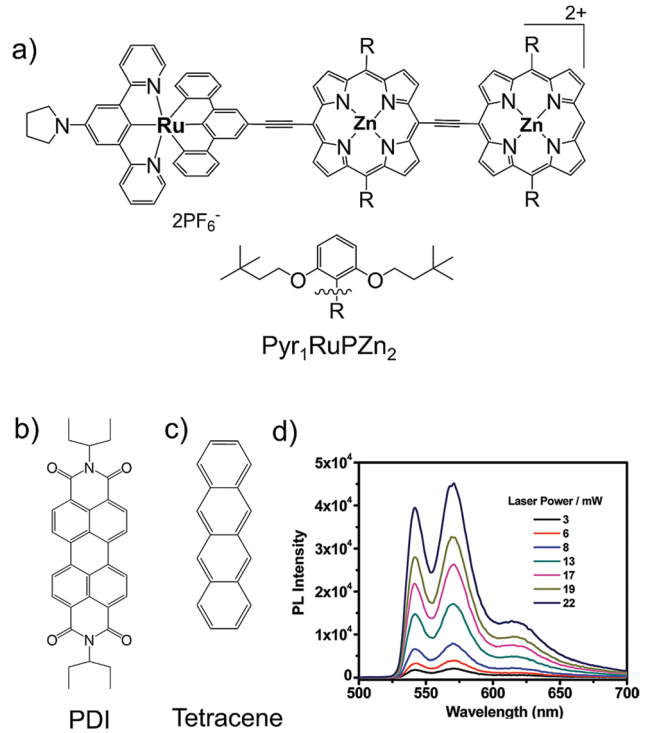

Fig. 9 (a)–(c) Molecular structures of (a) Pyr_1RuPZn_2 (sensitizer), (b) PDI and (c) tetracene (annihilators). (d) Photoluminescence intensity profile of a freeze–pump–thaw degassed MTHF solution of Pyr1RuPZn2 (3.3 μM) and PDI (420 μM) measured as a function of 780 nm incident laser power density.[28] Reproduced with permission from ref. 28. Copyright 2008, American Chemical Society.

promising strategy, these early systems had some shortcomings like, poor Φ_{UC} = 0.005% (808 nm excitation), absorption of sensitizer in the upconversion wavelengths region and high excitation intensities required for UC. They cited poor triplet energy transfer from NC to rubrene as the reason for low performance. It was partly due to tunnelling barrier caused by the long chain fatty acid used to stabilize the nanocrystal and limited encounter between diffusing NCs and rubrene for effective triplet energy transfer in the solution. To counter these issues, they demonstrated a new strategy of molecular engineering the nanocrystal with so-called "triplet transmitter ligands" by conjugating CdSe nanocrystals with anthracene in a Vis to Vis TTA-UC upconversion scheme using diphenyl anthracene as annihilator.[34] Tang's research group extended the triplet transmitter concept to NIR (808 nm) light harvesting by synthesizing 4-(tetracene-5-yl)benzoic acid (CPT) as transmitter, conjugated to PbS/PbSe nanocrystals with $\Delta E_{UC} \sim 0.65$ eV (808 nm to 568 nm) (Fig. 14c).[35] The triplet energy level of the transmitter were in between the sensitizer and annihilator. This resulted in 81 times enhancement of UC quantum yield of PbS–CPT–rubrene system to Φ_{UC} = 0.85% and 11 times enhancement for PbSe–CPT–rubrene system to Φ_{UC} = 1.05% in degassed toluene solution, compared with PbS–rubrene and PbSe–rubrene systems without the transmitter ligand.[35]

Subsequently, Tang's research group introduced PbS–CdS core shell nanocrystals (sensitizer), conjugated to 5-carboxylic tetracene (5-CT) as transmitter and rubrene (annihilator) system showing energy upconversion with ΔE_{UC} = 0.67 eV (808 nm to 561 nm), and record Φ_{UC} = 4.2 ± 0.5% at subsolar irradiance of

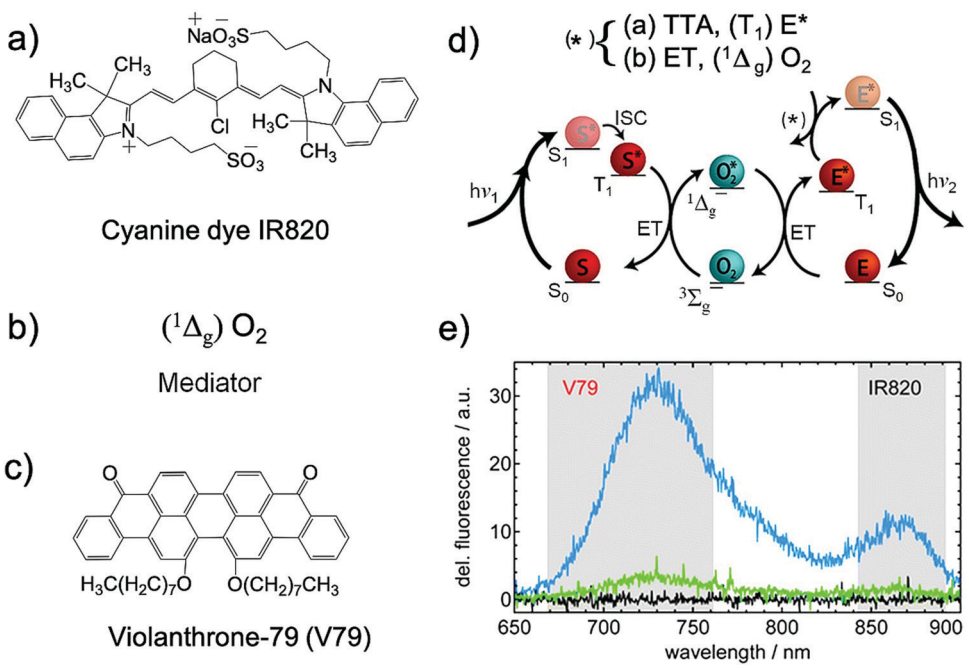

Fig. 10 (a)–(c) Molecular structures of (a) IR820 (sensitizer), (b) singlet oxygen (transmitter) and (c) V79 (annihilator). (d) Pathway of singlet oxygen mediated upconversion and (e) dependence of the delayed fluorescence signal on the oxygen concentration in DMF solution containing 1.7×10^{-3} M IR820 and 2.4×10^{-3} M V79 (signal integrated from 100 ns to 50 μs after the 830 nm excitation pulse, P = 6 μJ). The black, green, and blue spectra correspond to degassed, untreated, and oxygenated solutions, respectively. Reproduced with permission from ref. 29. Copyright 2011, American Chemical Society.

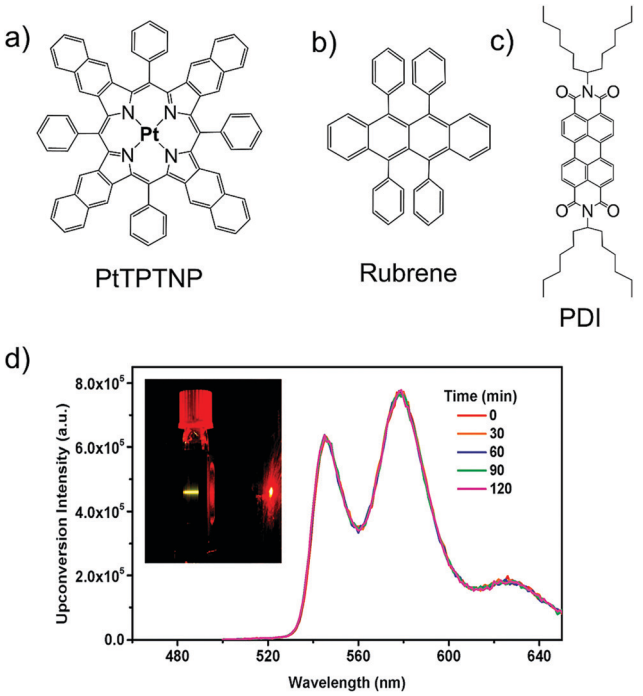

Fig. 11 (a)–(c) Molecular structure of (a) PtTPTNP (sensitizer), and (b) rubrene, (c) PDI (annihilators). (d) Upconverted emission spectra of 1.7 mM PtTPTNP and 0.14 mM PDI solution in deaerated toluene during continuous 690 nm excitation (30 W cm^{-2}). Inset: Photograph of the sample during photoexcitation at 690 nm. Reproduced with permission from ref. 30. Copyright 2013, The Royal Society of Chemistry.

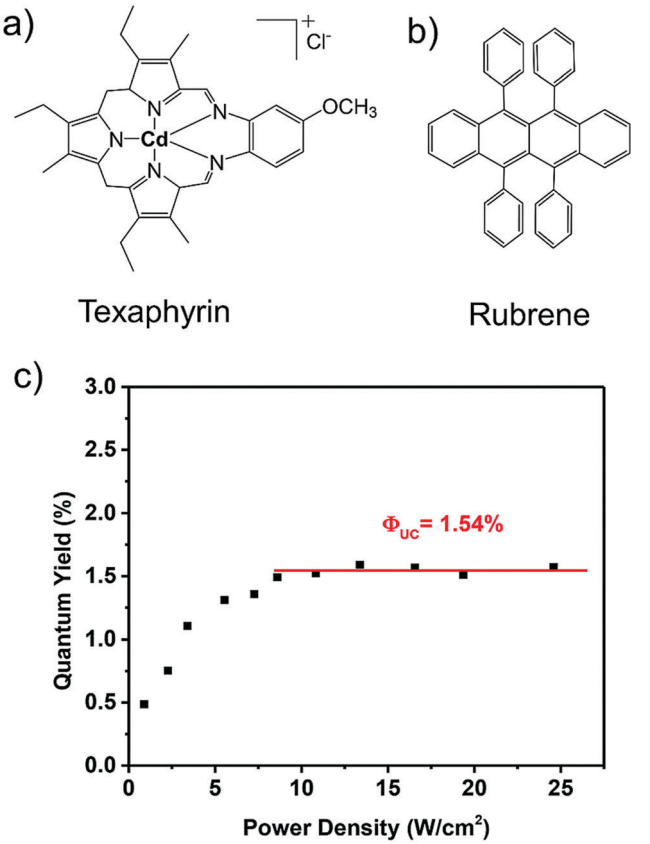

Fig. 12 (a) and (b) Molecular structures of (a) Texaphyrin (sensitizer), (b) rubrene (annihilator). (c) Upconversion quantum yields with 21 μM TXP and 0.33 mM rubrene in deaerated dichloromethane measured as a function of 680 nm incident light power density. Reproduced with permission from ref. 32. Copyright 2014, The Royal Society of Chemistry.

3.2 mW cm^{-2} in degassed toluene solution (Fig. 14d).[36] Introduction of CdS passivated the trap sites on PbS surface, which resulted in enhanced triplet energy transfer to annihilator *via* transmitter and ultimately enhanced Φ_{UC} at the subsolar irradiance.[36]

However, enhancing the shell thickness resulted in an exponential decrease in Φ_{UC}, due to the increased Dexter tunneling barrier across sensitizer (PbS)–annihilator (rubrene). They also calculated the damping coefficient (β) between sensitizer–annihilator as a function of increased shell thickness as per the eqn (7)

$$k_{et} = k_0 \exp(-\beta d) \quad (7)$$

where, k_{et} is rate of Dexter energy transfer between sensitizer and annihilator, and d is separation between sensitizer and annihilator. The empirical β was calculated to be 3.4 ± 0.1 $Å^{-1}$ which indicated large barrier height and energy offset between sensitizer and annihilator. They suggested that shell materials with lower bandgaps than CdS should be utilized for PbS cores to reduce the β in quest of enhancing quantum yield.[36]

In a later development, the hybrid inorganic core shell nanocrystal sensitizer concept was extended to Vis to UV TTA-UC using CdS/ZnS (sensitizer), naphthoic acid (transmitter) and 2,5-diphenyloxazole (annihilator). This system showed efficient upconversion (405 nm to 355 nm) with Φ_{UC} = 2.6 ± 0.25%, thus generalizing the concept to whole spectral range (NIR to Vis to UV).

One attractive feature of the QD sensitizers is that they can be prepared using (relatively) simple synthesis to match a broad range of energies. However, the QD/annihilator pairs presented above also exhibit certain challenges such as, difficulty to harvest NIR photons below 1.2 eV (1033 nm) due to inability of tetracene as transmitter to accept energy below 1.2 eV and triplet energy losses of ~200 meV during transmission from the QD to the annihilator, which makes them inefficient to increase the efficiency of commercial crystalline silicon solar cells (band gap = 1.12 eV).[15] To counter these challenges, Akshay Rao's research group, introduced a new annihilator, 5,11-bis(triethylsilylethynyl)anthradithiophene (TES-ADT), which acted as both transmitter and annihilator when coupled with PbS quantum dot (QD) sensitizers (Fig. 15).[15] The PbS QD showed significant triplet energy transfer (TET) to TES-ADT indicated by TET rate constant (k) of $k \approx 2 \times 10^8$ s^{-1}, assigned to the association of thiophene group of TES-ADT with PbS QD, thus avoiding the transmitter loss channel.

The PbS QDs-TES-ADT showed energy upconversion with ΔE_{UC} = 0.86 eV (1064 nm to 610 nm) in deoxygenated toluene solution. It was for the first time that NIR photons with energies as low as ~1.17 eV (1064 nm) were harvested. However, despite avoiding the transmitter loss channel, the

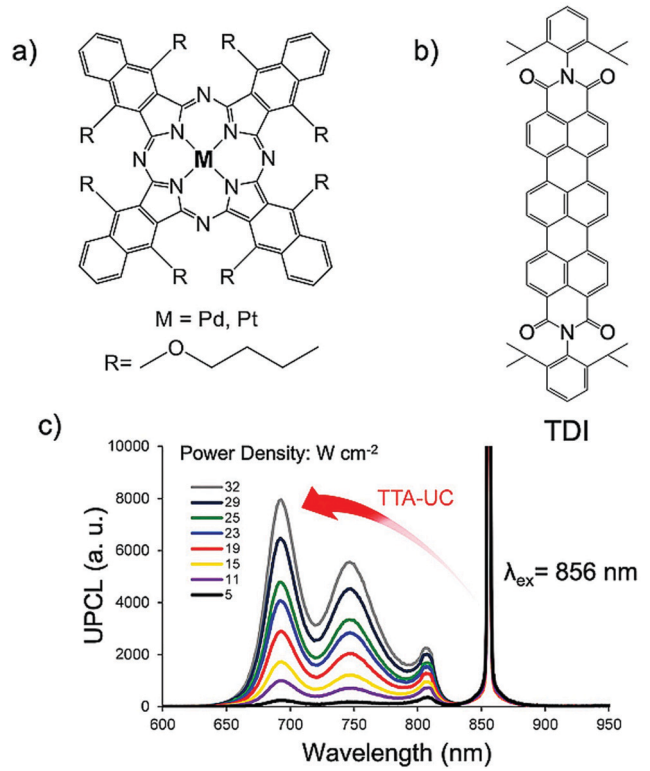

Fig. 13 (a) and (b) Molecular structures of (a) PtNac and PdNac, (b) TDI. (c) Upconverted emission spectra of the PtNac-TDI pairs in deaerated 1,2-DCB with different excitation power density of the 856 nm laser. Reproduced with permission from ref. 33. Copyright 2015, The Royal Society of Chemistry.

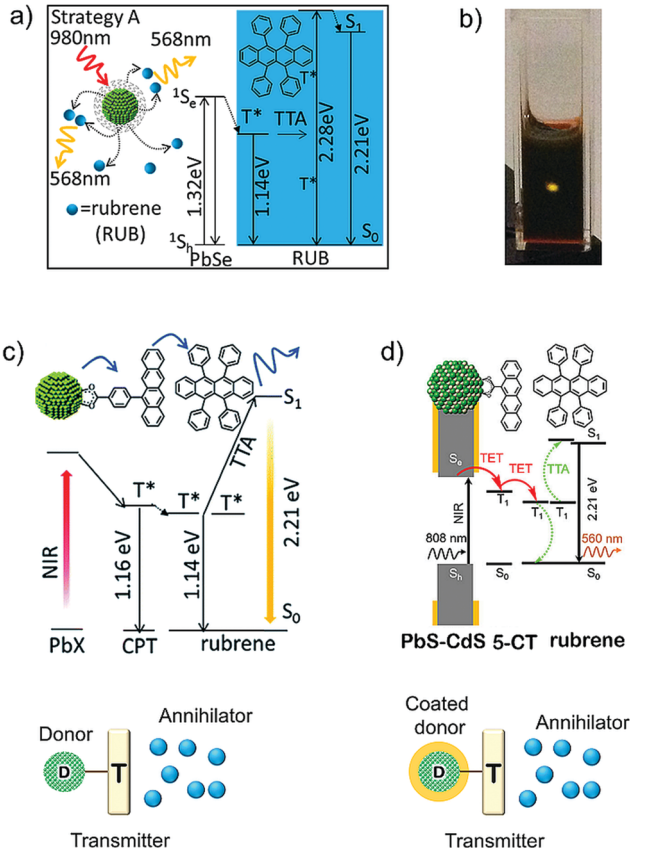

Fig. 14 (a) Schematic illustration of inorganic–organic hybrid upconversion in the organic ligands where the electronically inert PbSe nanocrystal (NC) transferred triplet energy directly to the triplet state of the organic annihilator rubrene.[34] (b) Photograph of upconversion in a cuvette containing the 2.1 nm PbSe/rubrene mixture. The yellow spot is emission from the rubrene originating from an unfocused cw 800 nm laser with an intensity of 1 W cm^{-2}. (c) Schematic of energy transfer during upconversion in the hybrid system with PbX (X = S, Se) as sensitizer, CPT as transmitter and rubrene as annihilator.[35] (d) Schematic of the energy transfer in PbS–CdS core–shell nanocrystal (NC) sensitizer. NC absorb the near-infrared photons. 5-CT is the transmitter ligand bound to the surface of the NCs that mediates TET from the NC to the rubrene annihilator. Rubrene then undergoes TTA to upconvert light, producing high-energy photons in the visible region.[36] Reproduced with permission from ref. 34–36. Copyrights, 2015 American Chemical Society (ref. 34), 2016 The Royal Society of Chemistry (ref. 35) and 2016 American Chemical Society (ref. 36).

PbS QDs-TES-ADT showed poor Φ_{UC} of 0.047%. They cited detachment of TES-ADT from PbS surface after TET, as the reason for this, which resulted in poor triplet energy transfer to diffusing TES-ADT molecules in the solution.[15]

In a new development, Schmidt's research group published the first report on photochemical upconversion of NIR light from below the silicon bandgap (1.12 eV) using PbS nanocrystals (NC) as sensitizer, violanthrone derivative (V79) as annihilator and singlet oxygen as mediator (Fig. 16).[37] The aerated solution of PbS/V79 showed delayed UC emission at 700 nm (ΔE_{UC} = 0.68 eV) upon 1140 nm laser excitation. No UC emission in the absence of oxygen indicated singlet oxygen mediated upconversion mechanism (Fig. 16a). However, the PbS-$^1O_2$-V79 solution showed very low UC quantum yield due to the difficulty of harvesting the energy from PbS NC.[37]

To counter this problem, they incorporated an energy trapping agent, 6,11-bis(triisopropylsilylethynyl)tetracene-2-carboxylic acid (TTCA) on the PbS NC surface to improve the harvesting of triplet energy from PbS NC (Fig. 16c). The Φ_{UC} was certainly improved to 0.015%, however at the expense of anti-Stokes shift. The deaerated PbS-TTCA/V79 solution was excited with 808 nm laser resulting in TTA-UC emission by V79 at 700 nm ($\Delta E_{UC} \sim$ 0.24 eV). The TTA mechanism in this system was demonstrated by the application of magnetic field which resulted in 7% decrease of UC emission at 300 mT. The magnetic field reduced the number of triplet pair states exhibiting singlet character due to the transformation of triplet eigen states, thus ultimately affecting the f factor. Interestingly, the introduction of oxygen into PbS-TTCA/V79 solution increased the upconversion intensity by 10 to 31-fold upon 930 nm laser excitation, which also became insensitive to the magnetic field effects. They reasoned change in the upconversion mechanism from TTA to sequential energy transfer from $^1\Delta_g$ O_2 for this behavior (Fig. 16d). Moreover, insensitivity to magnetic field was explained by a large zero-field splitting of the $^3\Sigma_g^-$ O_2, which did not affect the triplet sublevels by the moderate fields (300 mT) employed for analysis.[37]

However, the strong absorption of visible light by inorganic NCs still remains an outstanding issue, if we consider upconversion into

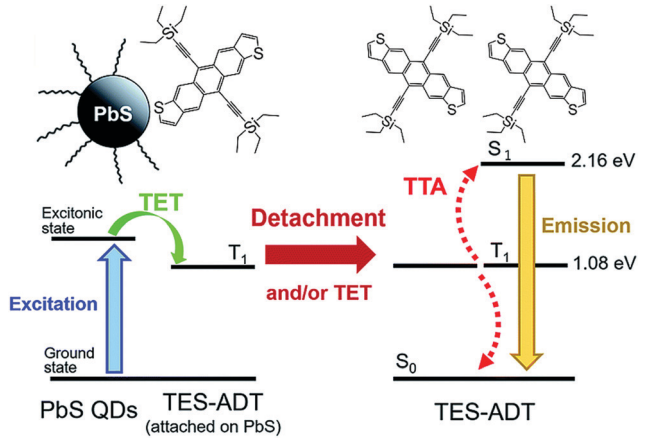

Fig. 15 Schemes of TTA-UC with PbS QDs as the triplet sensitizer and TES-ADT as an annihilator showing sequential energy transfer process for TTA-UC emission upon excitation of PbS QDs at 1064 nm. Reproduced with permission from ref. 15. Copyright 2019, The Royal Society of Chemistry.

whole visible region, it causes the reabsorption of the upconverted light by sensitizer resulting in poor UC quantum yield in typical experimental geometries. Synthesizing quantum dots with clear optical window by tuning their size and dimensions can be a potential solution. Moreover, transformation of below silicon band gap upconverting system to solid state devices would accomplish its practical goal of thwarting the Shockley Quiesser limit. In this direction the synthesis of new annihilator other than Violanthrone 79 with better photoluminescence quantum yield and non-aggregating nature in solid state are also sought.

3.2. Direct S_0-to-T_1 absorbing sensitizer based NIR to Vis molecular TTA-UC

In 2016, Kimizuka and Yanai's research groups introduced the direct S_0-to-T_1, absorbing osmium complexes as new NIR sensitizer, to minimize the energy loss during S_1-to-T_1 ISC of molecular sensitizers in TTA-UC (Fig. 17a, b, see also Fig. 1b).[38] The lipophilic osmium complex (Fig. 17c), showed a strong singlet–triplet MLCT (metal to ligand charge transfer) absorption band at 880 nm with ε = 3200. The small Stokes-shift of sensitizer upon 880 nm excitation indicated the absence of intersystem crossing. The mixed solution of sensitizer and rubrene upon excitation with 938 nm laser showed energy upconversion with ΔE_{UC} = 0.86 eV (938 nm to 570 nm) in deoxygenated dichloromethane solution (Fig. 17d). However, the developed system showed low Φ_{UC} = 0.0024%, due to low TTET from sensitizer to rubrene due to the small phosphorescence lifetime of sensitizer (τ_p = 12 ns).[38]

In 2017, Kimizuka and Yanai's research groups further expanded the concept of direct S_0-to-T_1 absorbing sensitizer to NIR to blue TTA-UC by using a new sensitizer, $Os(bptpy)_2^{2+}$ and tetra(*tert*-butyl)perylene (TTBP) as an annihilator.[39] The $Os(bptpy)_2^{2+}$/TTBP couple showed energy upconversion with ΔE_{UC} = 0.97 eV (724 nm to 462 nm) in deaerated dimethylformamide (DMF) solution. (Fig. 18c). When compared to previously reported system,[38] the $Os(bptpy)_2^{2+}$/TTBP couple showed an improved Φ_{UC} of 1.35%,[39] for not much different ΔE_{UC} (0.86 eV).[38] The reason for this improvement was due to the extended phosphorescence lifetime of new S_0-to-T_1 sensitizer (τ_p = 207 ns), resulting in an increased TTET efficiency from sensitizer to annihilator. This observation illustrates the

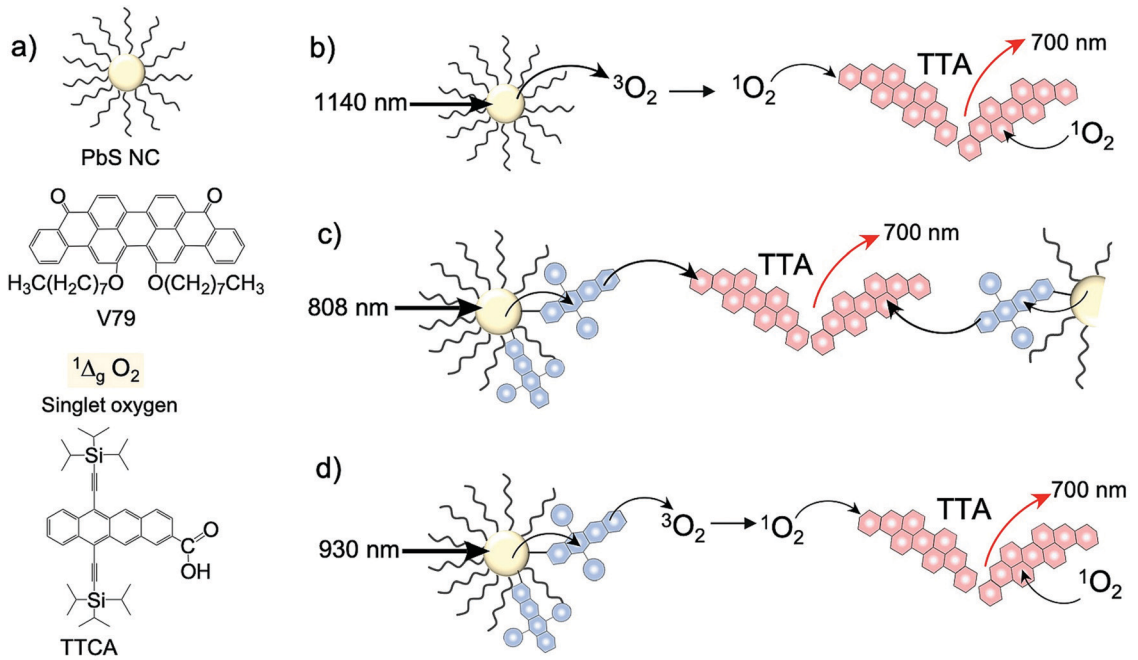

Fig. 16 (a) Structures of PbS nanocrystal (sensitizer), V79 dye (annihilator), $^1\Delta_g$ O_2 (mediator) and TTCA (energy trapping agent). (b) Pictorial representation of the mechanism of singlet oxygen mediated TTA-UC from below silicon band gap at 1140 nm laser excitation, (c) the mechanism of TTA-UC in PbS-TTCA/V79 in deaerated solution (λ_{ex} = 808 nm laser) and (d) sequential energy transfer mechanism of $^1\Delta_g$ O_2 leading to TTA-UC in aerated PbS-TTCA/V79 solution (λ_{ex} = 930 nm laser). Reproduced with permission from ref. 37. Copyright 2020, Springer Nature Limited.

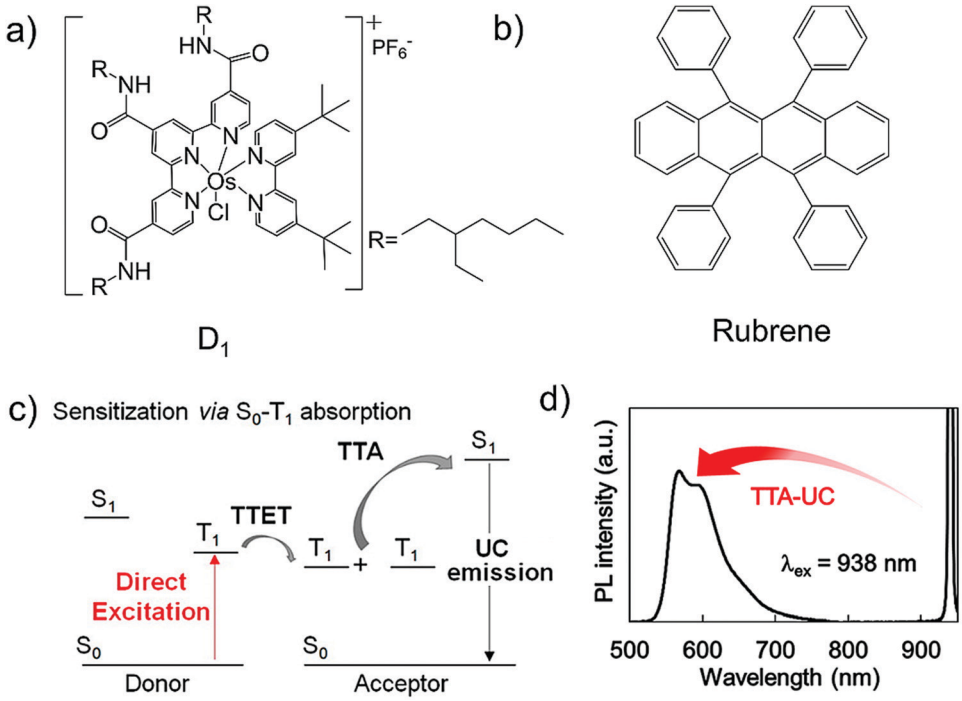

Fig. 17 (a) and (b) Molecular structures of (a) sensitizer, osmium complex (D_1) and (b) annihilator, rubrene. (c) TTA-based UC utilizing S_0-to-T_1 absorption of sensitizer. The absence of energy loss due to ISC allows the large anti-Stokes shift from NIR to visible. (d) Upconverted emission spectrum of the D_1–rubrene pair in deaerated DCM ([D_1] = 0.1 mM, [rubrene] = 5 mM, λ_{ex} = 938 nm, 780 nm short pass filter).[38] Reproduced with permission from ref. 38. Copyright 2016, American Chemical Society.

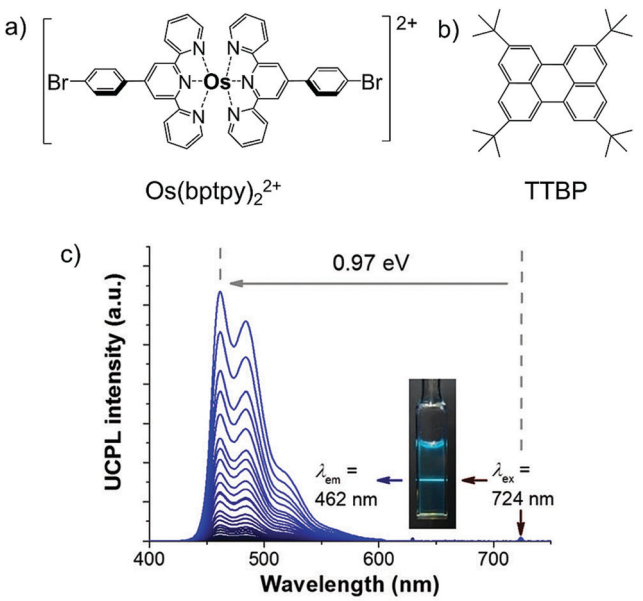

Fig. 18 (a) and (b) Molecular structures of (a) $Os(bptpy)_2^{2+}$ (S_0-to-T_1 sensitizer), and (b) TTBP (annihilator) (c) photoluminescence spectra of $Os(bptpy)_2^{2+}$ (20 μM) and TTBP (2 mM) in deaerated DMF with various excitation intensities from 132 mW cm^{-2} to 16.5 W cm^{-2} (λ_{ex} = 724 nm, 610 nm short pass filter).[39] Reproduced with permission from ref. 39. Copyright 2017, The Royal Society of Chemistry.

importance of long phosphorescence lifetime of S_0-to-T_1 sensitizer for high Φ_{UC} of NIR to Vis, TTA-UC systems.[39]

Kimizuka and Yanai's research groups further validated their concept of the "longevity of sensitizer's phosphorescence lifetime for an efficient TTA-UC" by developing a new S_0-to-T_1 sensitizer, $Os(peptpy)_2^{2+}$, with a long phosphorescence lifetime of 24 μs, resulting in an increase in Φ_{UC} to 2.95% with TTBP as an annihilator, with almost similar energy upconversion of ΔE_{UC} ~ 0.85 eV (724 nm to 484 nm) (Fig. 19).[6] For this they smartly functionalized the sensitizer osmium(II) bis(4′-phenyl-2,2′:6′,2″-terpyridine) ($Os(ptpy)_2$) having T_1 = 1.63 eV with phenyl-perylene (pPe) having T_1 = 1.50 eV for intramolecular triplet energy transfer (IMET). The $Os(peptpy)_2^{2+}$, showed thermally activated delayed phosphorescence at room temperature, resulting in an increased phosphorescence lifetime to 24 μs.[6]

Besides adjusting the phosphorescence lifetime of S_0-to-T_1 sensitizer, Kimizuka and Yanai's groups have recently demonstrated that tuning their triplet energy level closer to the triplet energy level of annihilator can also enhance the sensitizer to annihilator triplet energy transfer (TET) to enhance the UC efficiency.[40] For this they synthesized a new S_0-to-T_1 sensitizer, $Os(tpy)_2^{2+}$ (T_1 = 1.71 eV) and new annihilator, 9,10-bis-(diisopropylsilyl)anthracene ($(i\text{-}Pr_2SiH)_2An$) (T_1 = 1.70 eV). Interestingly the silyl substitution decreased the HOMO–LUMO gap of anthracene due to Si–C, σ–π and σ*–π* conjugation, resulting in the decrease of T_1 from 1.84 eV in anthracene to 1.70 eV in $(i\text{-}Pr_2SiH)_2An$ (Fig. 20).

The $Os(tpy)_2^{2+}/(i\text{-}Pr_2SiH)_2An$ couple showed NIR to violet energy upconversion with an anti-Stokes shift of ΔE_{UC} = 1.28 eV (724 nm to 415 nm), crossing into the violet region for the first

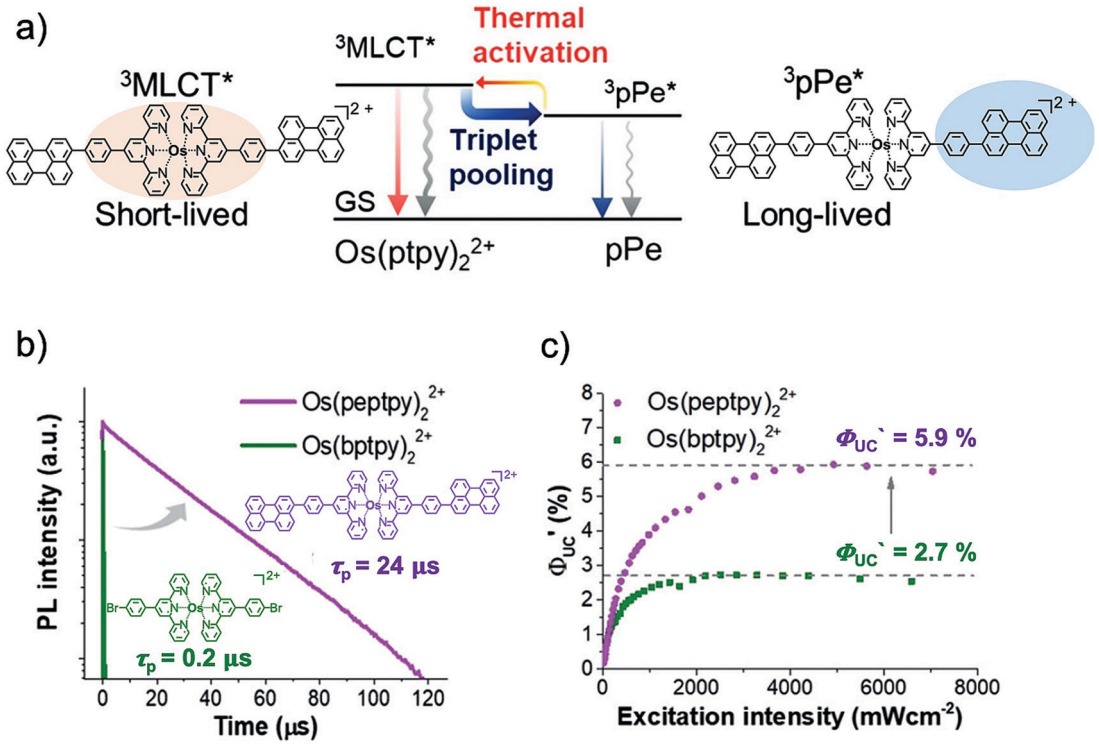

Fig. 19 (a) The mechanism of the triplet-lifetime extension and thermally activated delayed phosphorescence of Os(peptpy)$_2^{2+}$ (sensitizer). (b) Phosphorescence decays of Os(peptpy)$_2^{2+}$ (magenta, λ_{ex} = 498 nm, λ_{em} = 743 nm, 20 µM) and Os(bptpy)$_2^{2+}$ (green, λ_{ex} = 494 nm, λ_{ex} = 743 nm, 20 µM) in deaerated DMF. (c) Comparative UC quantum efficiency as a function of excitation intensity for Os(peptpy)$_2^{2+}$-TTBP (magenta) and Os(bptpy)$_2^{2+}$-TTBP (green) in deaerated DMF solution.[6] Reproduced with permission from ref. 6. Copyright 2019, Wiley-VCH Verlag GmbH & Co. KGaA, Weinheim.

time (Fig. 20). Moreover, the higher sensitizer to annihilator TET resulted in a record Φ_{UC} of 5.5% for such a long ΔE_{UC} of 1.28 eV in deaerated tetrahydrofuran solution.[40]

3.3. Lanthanide-organic complex sensitizer based NIR to Vis Molecular TTA-UC

Focusing on energy upconversion beyond 950 nm, recently Howard and Turshatov's research groups introduced lanthanide-organic complex as NIR sensitizers. Citing the shortcoming of "upconversion reabsorption" by inorganic nanocrystals, they suggested a β-diketonate complex of ytterbium (Yb-L), as a suitable alternative on grounds of its clear optical window in the 500 nm to 900 nm region and phosphorescence lifetime of 10 µs (Fig. 21). Upon excitation with 980 nm laser, the Yb-L/rubrene couple in deoxygenated deuterated tetrahydrofuran showed energy upconversion with ΔE_{UC} = 0.95 eV (980 nm to 559 nm) and Φ_{UC} of $< 0.5\%$.[41]

However, besides the advantage of clear optical window, several limitations of Yb-L sensitizer were also highlighted such as poor Φ_{UC}, high excitation intensity and requirement of deuterated solvents. The deuterated solvent was required to avoid nonradiative deactivation by multiphoton relaxation *via* energy transfer to vibrational overtones of high-energy, highly anharmonic oscillators (mostly stretching modes of X–H moieties with X = O, N, C) in the vicinity of the metal.[41]

Even after being highly prone to photo-degradation, rubrene has been the main annihilator in most of the NIR to Vis TTA-UC systems. Kazlauskas's research group investigated the low Φ_{UC} of metallophthalocyanine sensitized rubrene systems based on the subsequent energy transfer steps. Upon investigating, the Pd(II) phthalocyanine/rubrene pair in deoxygenated toluene, they concluded that the low statistical probability (f = 15.5 ± 3%) of getting rubrene's singlet from two triplets after TTA is the key limiting factor for its poor UC quantum yield.[18] The low f value sets the maximum limit of 8% for Φ_{UC} with rubrene based TTA-UC systems. They investigated different sensitizer/annihilator couples and examined their comparative quantum yield considering f factor. The obtained maximum Φ_{UC} for the Pd(II) phthalocyanine (PdPc)/rubrene couple (Φ_{UC} = 5.6%), was followed by Pt(II) phthalocyanine (PtPc)/rubrene couple (Φ_{UC} = 4.9%) and Pd(II) phthalocyanine (PdPc)/tertiary butyl-rubrene couple (Φ_{UC} = 1.3%) after reabsorption correction upon 730 nm excitation. Therefore, besides poor photostability, they highlighted another limiting factor of low f value of rubrene based TTA-UC system.[18]

One possible application of TTA-UC systems, is in photovoltaics to harvest the wasted sub-band gap photons to enhance the efficiency.[1–3] Schmidt's research group were the first to demonstrate the integration of red to yellow (670 nm to 570 nm) TTA-UC system of PQ_4PdNA/rubrene couple to organic bulk heterojunction solar cells (OPV), hydrogenated amorphous silicon (a-Si:H) thin-film solar cell and dye sensitized solar cells (DSC) (Fig. 22a and b)[1,2] They measured a peak efficiency

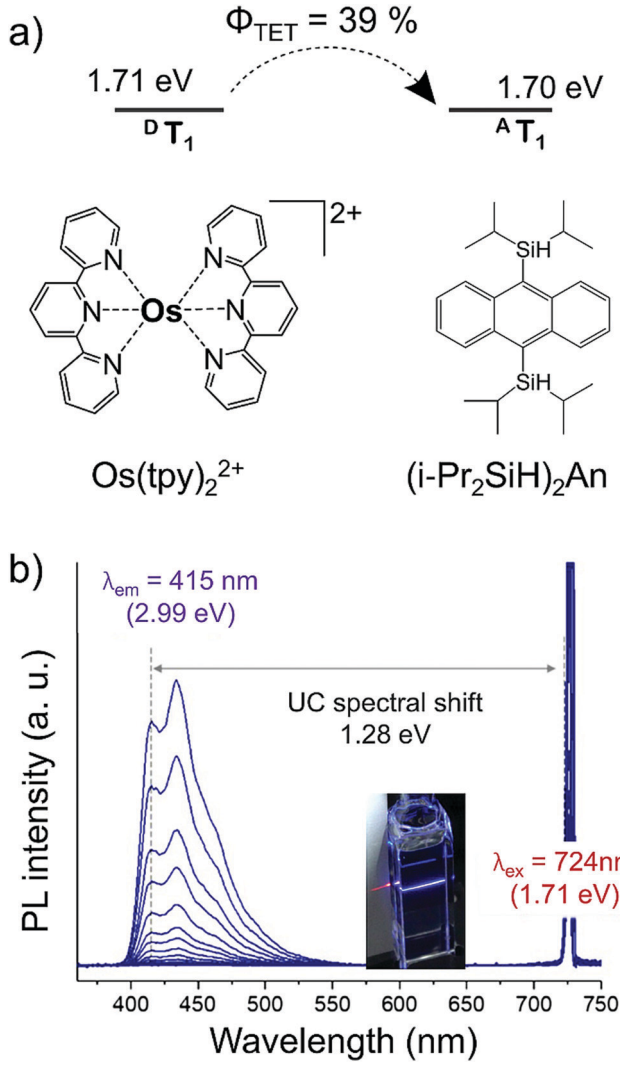

Fig. 20 (a) Molecular structures of $Os(tpy)_2^{2+}$ (sensitizer), and $(i\text{-}Pr_2SiH)_2An$ (annihilator), and schematic of efficient triplet energy transfer due to close triplet energy levels. (b) Photoluminescence (PL) spectra of $(i\text{-}Pr_2SiH)_2An$ (0.50 mM) and $Os(tpy)_2^{2+}$ (20 μM) in deaerated THF at various excitation intensities λ_{ex} from 0.19 W cm^{-2} to 247 W cm^{-2} (λ_{ex} = 724 nm, 610 nm short-pass filter). Inset, showing photograph of the THF solution of $(i\text{-}Pr_2SiH)_2An$ (40 mM)-$Os(tpy)_2^{2+}$ (20 μM) under the excitation at 724 nm without a filter.[40] Reproduced with permission from ref. 40. Copyright 2020, The Royal Society of Chemistry.

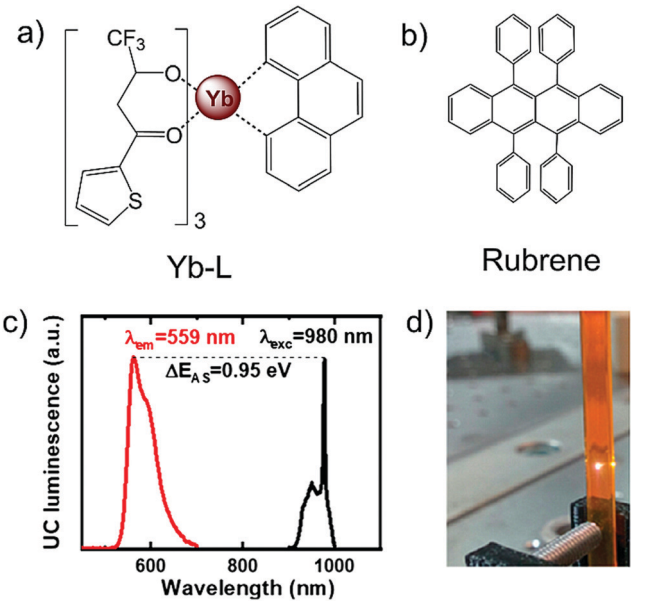

Fig. 21 (a) and (b) Molecular structures of (a) Yb-L (sensitizer) and (b) rubrene (annihilator). (c) UC luminescence of rubrene excited with a 980 nm laser (maroon line). Excitation spectrum of TTA-UC, laser intensity maintained at 100 W cm^{-2} (black line). (d) Unfiltered photograph of UC luminescence (λ_{exc} = 980 nm, 300 W cm^{-2}).[41] Reproduced with permission from ref. 41. Copyright 2020, American Chemical Society.

enhancement of (1.0 ± 0.2)% at 720 nm, under irradiation equivalent to (48 ± 3) suns (AM 1.5) for a-Si:H p–i–n/UC device (Fig. 22a) and enhanced figure of merit of 2.5×10^{-4} mA cm^{-2} in response to light in the region of 600–750 nm using pump beam intensity as low as ~3 equivalent suns for DSC/UC device (Fig. 22b).

However, most of the solar cells integrated TTA-UC systems are based on sensitizer/annihilator couples dissolved in deoxygenated organic solvents.[1–3] Such solution based systems serve as proof of concept demonstration, yet, practical applications in optoelectronics and solar cells demand their efficient functioning in liquid crystalline or solid state. In the next section we will discuss the developments in liquid crystalline/solid state NIR to Vis TTA-UC systems including both inorganic nanocrystals and molecular sensitizers.

3.4. NIR to Vis molecular TTA-UC in liquid crystals

Kimizuka, Yanai and Sagara's research groups further expanded the applications of NIR to Vis TTA-UC to molecular thermo-photoswitching in liquid crystals. Using an asymmetric luminescent cyclophane, 9,10-bis(phenylethynyl)anthracene unit-based annihilator (Fig. 23a), doped with S_0-to-T_1 sensitizer, $Os(bptpy)_2^{2+}$ (Fig. 18a), they reported proof-of-concept demonstration of thermal responsive dual UC emission upon 730 nm laser excitation (Fig. 23b–d).[20] It was possible due to the thermoreversible photo-emissive characteristics of cyclophane annihilator upon phase transition. The annihilator changes to kinetically trapped Y-phase (yellow emissive) and thermodynamically stable crystalline G-phase (green emissive) upon rapid and slow cooling of nematic liquid crystalline phase to room temperature. Well, the S_0-to-T_1 sensitizer doped Y-form showed yellow UC emission, which changed to green UC emission due to the phase transition to G-form upon annealing the Y-form at 80 °C.[20]

The liquid crystalline matrix can provide orientational control for directed emission by chromophores, which can channelize the upconverted singlet energy better when applied to a device like solar cells in order to minimize the energy loss. Our research group has published a proof-of-concept demonstration of directed photon upconversion emission (Visible to Visible) by dissolving sensitizer/annihilator couples of palladium(II) octaethylporphyrin/anthracene derivatives in orientationally ordered nematic liquid crystalline matrix (Fig. 24).[21] We obtained controlled switching of directional

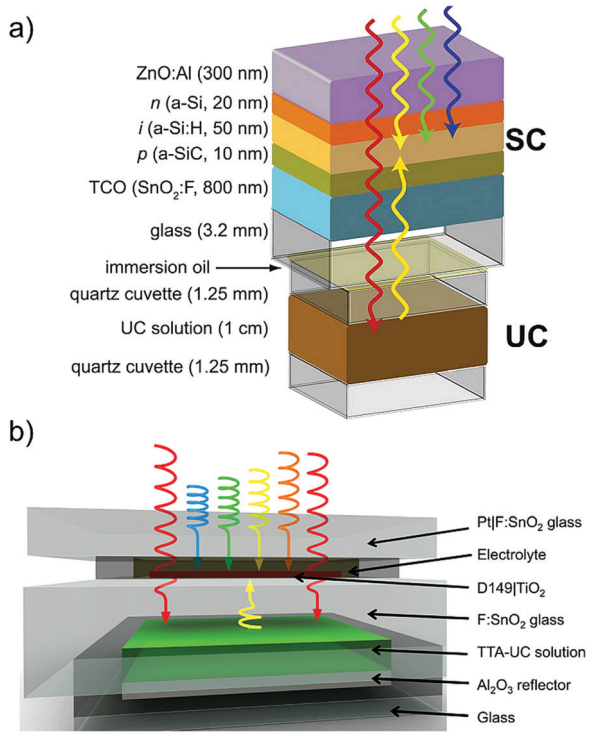

Fig. 22 Cartoon of the integration of TTA-UC solution to (a) hydrogenated amorphous silicon thin film solar cells (a-Si:H) and (b) dye sensitized solar cells (DSC). Low-energy photons pass through the active layer of the device and cause TTA-UC in the TTA-UC layer. Upconverted photons that are absorbed by the active layer provide extra current to the device.[1,2] (a) Reproduced with permission from ref. 1 Copyright 2012 and (b) from ref. 2 Copyright 2012 American Chemical Society.

TTA-UC emission with a ratio of 0.37 (for 9-(4-cyanophenyl), 10-phenylanthracene annihilator) between axial and longitudinal emission direction and with 1.52 directivity, which is near to the theoretical maximum of 2 obtained for perfectly oriented samples.[21] We think that this strategy, can be extended by suitable selection of NIR to Vis chromophores, either by transforming them to liquid crystals or by dissolving in suitable liquid crystal for directional channelization of upconverted emission.

4. Solid state NIR to Vis molecular TTA-UC

In addition to oxygen quenching of triplets and fabrication challenges, aggregation of chromophores is one key obstacle to achieve efficient NIR to Vis TTA-UC in solid state devices. While moving from Vis to NIR region, the increased π electron density of chromophores *via* extending conjugation along aromatic structures enhances the propensity of aggregation. Besides photoluminescence quenching, aggregation causes many secondary issues such as poor sensitizer to annihilator TET, quenching of annihilator triplet by trap sites, intermolecular reactions and back energy transfer *etc.* Nevertheless, different strategies have been developed over the years to address these issues.

For example, Bulović, Bawendi and Baldo's research groups introduced the emitter concept, which consists of an additional emitter component along with the conventional sensitizer/annihilator couple.[42] They reported NIR to Vis solid thin film comprising, PbS colloidal nanocrystals as a sensitizer, rubrene as an annihilator and dibenzotetraphenylperiflanthene (DBP) as an emitter (Fig. 25).[42]

The PbS–rubrene–DBP thin film showed energy upconversion with $\Delta E_{UC} \sim 0.49$ eV (808 nm to 612 nm) upon 808 nm excitation. Interestingly, the addition of DBP as a guest in the rubrene host increased the upconverted photoluminescence by a factor of 19 leading to an $\Phi_{UC} = 0.6 \pm 0.1\%$ at an excitation intensity of half sun. It was a significant development to use the emitter, in order to circumvent the challenges with nanocrystal sensitizers of absorbing the upconverted light and rubrene aggregation to reduce the UC quantum yield. The upconverted singlet energy of rubrene is rapidly transferred to DBP *via* Förster resonance energy transfer to emitter before the NC could reabsorb it.[42]

Seeking further improvement in the Φ_{UC} of PbS–rubrene–DBP film, Bawendi's research group investigated the effect of PbS surface-passivating ligand's length (4C to 18C) as a barrier for effective TET between PbS and rubrene (Fig. 26).[12]

Besides this, they also improved the device structure by using additional optical spacer, tris(8-hydroxyquinoline) aluminum (AlQ_3) and a silver back reflector (Fig. 26a).[12] They found hexanoic acid (6C), as the best ligand for efficient TET from PbS to rubrene in solid state (Fig. 26b), which resulted in an improved $\Phi_{UC} = 3.5 \pm 0.5\%$ for $\Delta E_{UC} \sim 0.5$ eV (808 nm to 610 nm). They calculated the UC quantum efficiency using a modified eqn (8).[12,42]

$$\eta_{UC} = \frac{P_{\lambda=808\ nm}}{I_{\lambda=808\ nm} A_{\lambda=808\ nm}} \frac{I_{\lambda=450\ nm} A_{\lambda=450\ nm}}{P_{\lambda=450\ nm}} \times 2 \qquad (8)$$

η_{UC} denotes UC quantum efficiency, P denotes the number of visible photons emitted, I denote the number of photons in the incident laser beam, and A denotes the absorption by the active material at specific wavelength (λ = 808 nm and 450 nm). A factor 2 is multiplied with equation to calculate upconversion efficiency for 100% theoretical maximum.

Kimizuka and Yanai's research groups introduced a new strategy of translating the chromophores into amorphous nanoparticles to prevent aggregation in solid state. The osmium complex/rubrene couple (Fig. 17a and b),[38] nanoparticles (Fig. 27a) dispersed in polyvinyl alcohol (PVA) film (Fig. 27b) showed stable TTA-UC (938 nm to 570 nm) with a $\Phi_{UC} = 0.17\%$ (Fig. 27c).[38]

They applied the same strategy to prepare $Os(bptpy)_2^{2+}$/TTBP couple (Fig. 18a and b) nanoparticles, which upon dispersion in PVA film showed stable energy upconversion with $\Delta E_{UC} = 0.83$ eV (724 nm to 490 nm) in air, but with low $\Phi_{UC} = 0.055\%$ (Fig. 27d).[39] It was due to the decrease in fluorescence quantum yield of TTBP from 12% to 5.9% upon grinding which further decreased to 0.91% upon mixing with $Os(bptpy)_2^{2+}$ due to the formation of singlet defect sites. Further, annihilator to sensitizer back energy transfer also led to the low Φ_{UC}.

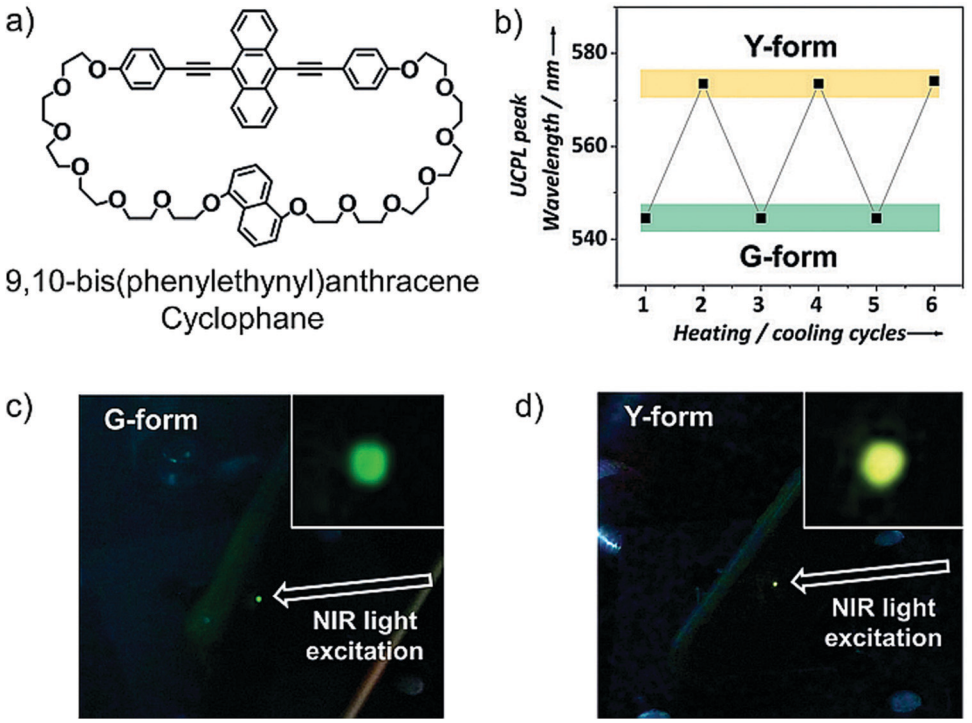

Fig. 23 (a) Molecular structure of 9,10-bis(phenylethynyl)anthracene based asymmetric cyclophane (annihilator). (b) Reversible switching of UC emission peak position by repeated heating and cooling cycles. (c) and (d) Photographs of 0.5 mol% $Os(bptpy)_2^{2+}$ (sensitizer) doped annihilator in the G-form (c) and the Y-form (d) irradiated by a 730 nm NIR laser. Reproduced with permission from ref. 20. Copyrights 2018, Wiley-VCH Verlag GmbH & Co. KGaA, Weinheim.

Kimizuka and Yanai's research groups also conceptualized that the annihilator MOF's of suitable pore sizes to fit the sensitizer can also prevent the sensitizer aggregation problem. Working on this strategy they succeeded to incorporate PbS nanocrystals into the diphenyltetracene containing metal organic framework (T-MOF) showing energy upconversion with $\Delta E_{UC} \sim$ 0.68 eV (785 nm to 550 nm), therefore presenting the first example of NIR to Vis TTA-UC MOF (Fig. 28a).[22] Further they also incorporated the S_0-to-T_1 sensitizer, $Os(tpyCOOH)_2^{2+}$ into a new annihilator-based MOF built from [4-((10-(4-carboxyphenyl)-anthracene-9-yl)ethynyl)benzoic acid] (CPAEBA) as shown in Fig. 28b.[23] The 1,3,5-tri(1-naphthyl)benzene blended Os-CPAEBA MOF film showed air stable energy upconversion with ΔE_{UC} = 0.58 eV (724 nm to 540 nm) as shown in Fig. 28c. However, low absolute Φ_{UC} = 0.006%, was observed due to the presence of possible triplet trap sites in the locally disordered structures of MOF. Alternatively, they also synthesized a silyl substituted anthracene to avoid annihilator aggregation (Fig. 20a). The degassed $Os(tpy)_2^{2+}$ doped $(i\text{-}Pr_2SiH)_2An$ solid powder showed largest NIR to violet energy upconversion of 1.15 eV upon 724 nm excitation, however with a low absolute Φ_{UC} = 0.01%.[40] It was due to the aggregation of sensitizer in the annihilator crystals, since no emission shift was observed between solution and solid state emission spectra of annihilator. The bulky silyl group minimized the interchromophore interactions to avoid annihilator aggregation.

Recently, Yamada's research group has reported a binary amorphous solid microparticles film formed from a new Pd-porphyrin sensitizer (PdTPTAP) and annihilator (rubrene) showing energy upconversion with $\Delta E_{UC} \sim$ 0.6 eV (785 nm to 570 nm) with an Φ_{UC} = 0.5% at low threshold excitation intensity of 100 mW cm^{-2} (Fig. 29).[43] Interestingly, the film was formed after simple drying of the THF solution of chromophores. Although, 100% sensitizer to annihilator TET, was reported, UC quantum yield was recorded low due to singlet fission promoted fluorescence quenching of rubrene and back energy transfer to the sensitizer in the solid state.[43]

To address the issue of singlet fission (SF), induced fluorescence quenching of rubrene, Kazlauskas's research group synthesized *t*-butyl substituted rubrene (*t*-butyl-rubrene) as shown in Fig. 30.[44] Interestingly, 20 times higher fluorescence quantum yield was observed for neat *t*-butyl-rubrene film compared to the rubrene film, indicating suppression of singlet fission upon substitution. However, on the negative side, the substitution with *t*-butyl group also introduced secondary adverse effects such as reduced diffusion and diffusion assisted TTA of rubrene, which ultimately affected the overall UC quantum yield. The Pd-phthalocyanine–*t*-butyl-rubrene–DPB (Sensitizer–annihilator–emitter) doped polystyrene film showed energy upconversion with ΔE_{UC} = 0.33 eV (730 nm to 610 nm) with an improved Φ_{UC} of 0.3% in comparison to rubrene (0.07%) due to the reduced singlet fission,[44] which is still not high enough to compete with other systems.

Grozema's research group has demonstrated the application of solid state NIR to Vis TTA-UC to dye sensitized solar cell.[45] The TTA-UC fabricated solar cell was comprised of a trilayer

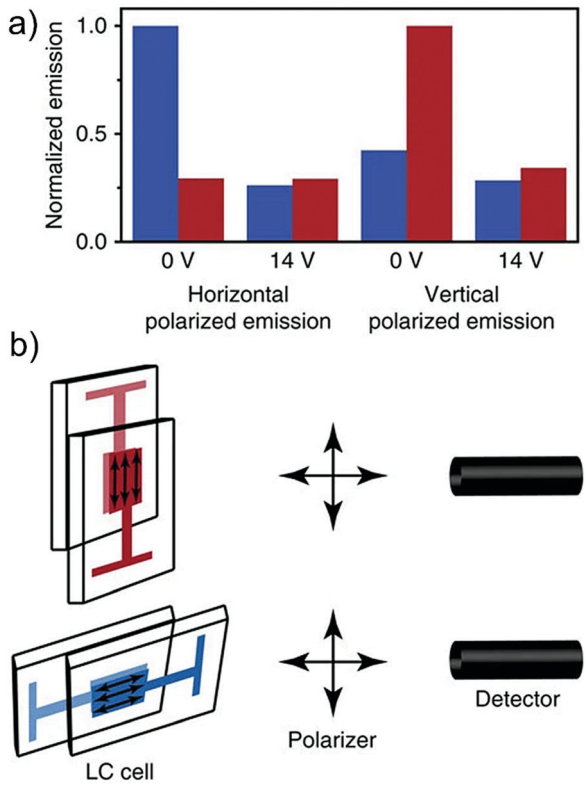

Fig. 24 Polarized upconverted emission. (a) Upconverted emission from an LC-cell with the LC matrix in a horizontal (blue) or vertical (red) position, at 0 or 14 V_{rms}, monitored through a polarizer in horizontal or vertical position for palladium(II)octaethylporphyrin/9-(4-cyanophenyl), 10-phenyl-anthracene couple. Excitation wavelength was 547 nm and the emission was monitored at 430 nm. (b) Schematic illustration of the setup of the experiment with the LC-cell either in a vertical (red) or horizontal (blue) position, and the emitted light monitored either through a vertically or horizontally positioned polarizer. Reproduced from ref. 21. It has a Creative Commons Attribution 4.0 International License. Copyrights 2016, Springer Nature Limited.

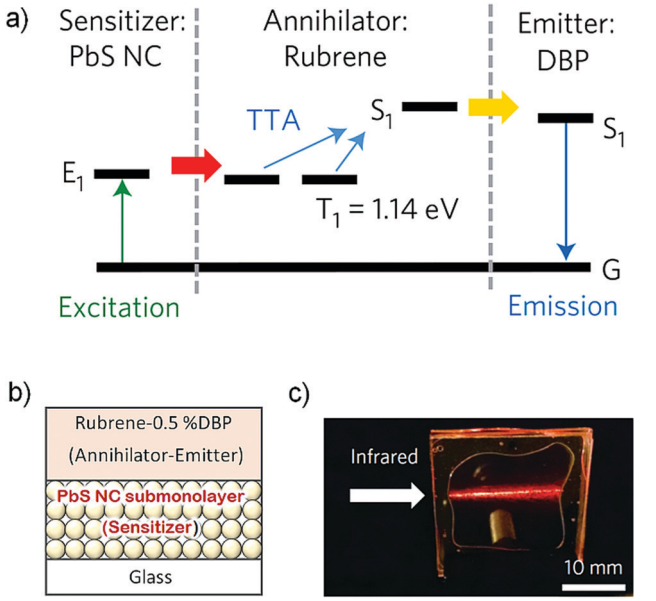

Fig. 25 (a) Schematic energy diagram showing the processes of triplet sensitization by the NCs, triplet–triplet annihilation in rubrene and emission from DBP (emitter). (b) The solid-state device structure of the thin film and (c) photograph showing DBP photoluminescence sensitized by λ = 850 nm NCs under excitation at λ = 808 nm. Reproduced with permission from ref. 42. Copyright 2015, Springer Nature Limited.

structure (sensitizer–annihilator-electron acceptor) wherein, crystalline layers of TTA-UC couple (fluorinated zinc phthalocyanine) (F_{16}ZnPc)/methyl substituted perylenediimide (PDI-CH_3) were deposited on a polycrystalline layer of TiO_2 (electron acceptor). The excitation of sensitizer layer with NIR light (700 nm), resulted in an injection of electron from upconverted singlet excited state of annihilator into the conduction band of TiO_2, measured by photoconductance signals (Fig. 31).[45] Although, the absorbed photon to injected electron efficiency for this system was low (1.8%), it provided a new route for practical fabrication of solid state TTA-UC to solar cells beyond deoxygenated organic solvents.[1,2]

The low UC quantum yield obtained with NIR to Vis solid state TTA-UC systems is one of the key issues impeding their integration to the photovoltaic devices. Further research in terms of new sensitizer and annihilator designs and concerted efforts in the demonstrated proof of concept systems are desired to increase the UC quantum yield. Moreover, their practical integration also requires developments in fabrication technique in terms of oxygen protection and molecular dispersion.

5. NIR to Vis molecular TTA-UC in photocatalysis

While the known photocatalysts need excitation by UV or Vis light with a typical excited-state energy of 2.18 eV (570 nm) to 3.47 eV (357 nm), it is possible to drive such catalytic processes under much lower energy irradiation by using photon upconversion. In this context, by exploiting the high penetration depth of NIR light (817 nm), Congreve, Rovis and Campos's research groups reported photoredox catalytic application of NIR to Vis TTA-UC systems comprising sensitizer/annihilator couples of palladium(II) octabutoxyphthalocyanine (PdPc)/furanyldiketopyrrolopyrrole (FDPP) and platinum(II) tetraphenyltetranaphthoporphyrin (PtTPTNP)/tetra-*tert*-butylperylene (TTBP).[4] The annihilators FDPP and TTBP were able to drive photocatalytic processes for a series of organic reactions *via* their upconverted orange and blue emissions under NIR light irradiation (Fig. 32).[4]

The obtained yields for all the reactions were found to be comparable to that obtained at high energy excitation of photocatalyst, thus demonstrating the relevance of NIR to Vis TTA-UC in energy economy. Interestingly, the annihilator TTBP could also act as photocatalyst, therefore simplifying the reaction further.

However, carrying out such reactions in aerated conditions remains a big challenge to reduce the synthesis cost. Therefore, there is a need to develop oxygen stable organic reaction medias such as efficient NIR to Vis TTA-UC organogels and microcapsules containing organic solvents that in confined domain can work as a viable solution.

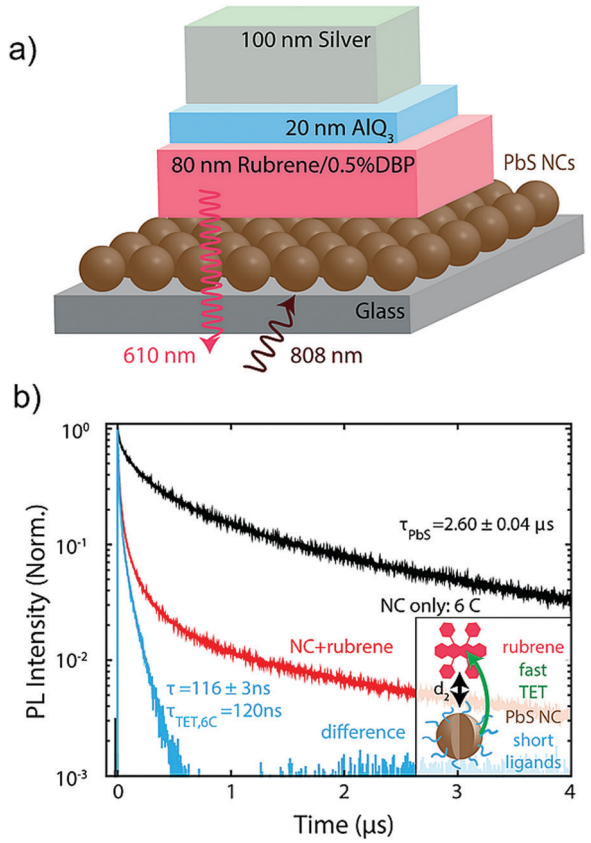

Fig. 26 (a) Solid state device structure comprising of 790 nm PbS NCs (sensitizer) and 80 nm rubrene (annihilator) doped with 0.5% DBP (emitter), an optical spacer made of 20 nm thick AlQ3 and a 100 nm thick silver back reflector. (b) Transfer dynamics for hexanoic acid (6C), with τ_{6C} = 116 ± 3 ns (light blue). This corresponds to a characteristic transfer time of τ_{TET}, 6C = 120 ns. Insets: Cartoons to highlight the enhanced transfer rate (reduced transfer time) when replacing long ligands with short ligands due to the reduced spacing d_2. Reproduced with permission from ref. 12. Copyright 2017, American Chemical Society.

6. Bio-applicable NIR to Vis molecular TTA-UC systems

Molecular TTA-UC systems have also been applied to biological applications, especially bioimaging. However, most of the reported systems are limited to Vis to Vis UC and there are scarce reports on NIR to Vis TTA-UC. This is due to the obvious reasons of solubility limitations of NIR dyes in aqueous environment due to enhanced hydrophobicity and dissolved oxygen in the water of body tissue. But it is highly appealing to exploit the non-invasive nature of NIR light in TTA-UC for *in vivo* applications like bioimaging, optogenetics, theranostics.[5,6]

To circumvent limitations of solubility and photostability, Li's research group dissolved (PdPc(OBu)$_8$/9,10-bis(phenylethynyl)-naphthacene) (BPEN) couple in reductive solvent soybean oil (Fig. 33).[5] The molecular structures of chromophores are shown in Fig. 32a and 6b. They hypothesized that reductive solvent consumes the generated singlet oxygen upon reaction of annihilator triplet with molecular oxygen thus increasing the photostability. Additionally, the edible and non-polar nature of soybean oil makes it a suitable solvent for the dissolution of dyes for biological applications. For bioimaging, they transformed the dyes dissolved in oil to upconversion nanoparticles (TTA-UCNCs) using bovine serum albumin/dextran as stabilizer at the oil water interface (Fig. 33a). The UCNCs showed stable upconversion emission at 610 nm upon 730 nm NIR laser excitation. UCNCs injected mouse showed TTA-UC emission between 575 to 700 nm upon excitation with a 730 nm laser, with signal to noise ratio of 15 (Fig. 33b).[5]

Kimizuka, Yanai and Ajioka's research groups reported an optogenetic application of NIR to blue hydrogel comprising, Os(peptpy)$_2^{2+}$/TTBP couple dispersed in Pluronic f127 micelles (Fig. 34a).[6] The molecular structure of sensitizer/annihilator is shown in Fig. 18b and 19a. Being a high temperature gelator, the O_2 blocking ability of hydrogel increased upon annealing at 80 °C, allowing stable functioning of TTA-UC in ambient environments. The UC hydrogel was applied for NIR light stimulation of the hippocampal dendritic spines involved in learning and long-term memory by receiving excitatory input from axons (Fig. 34b). Dendritic protrusions from the spine was observed with the UC hydrogel from 6 hours after the NIR-light stimulation indicating spine growth and thus demonstrating the optogenetic behavior (Fig. 34c and d).[6]

Recently Bao, Han and Xue's research groups published the application of NIR to Vis upconversion in mammalian Near-Infrared image vision by developing injectable photoreceptor-binding upconversion nanoparticles of β-NaYF$_4$: 20%Yb, 2%Er@β-NaYF$_4$ (980 nm to 535 nm).[46] These nanoparticles were stabilized with protein concanavalin A for binding to the outer segments of photoreceptors in the mouse retinae. A rod cells photocurrent was observed upon 980 nm light flash from nanoparticle injected mice whereas the rod cells from non-injected mice showed no responses, hence indicating NIR stimulated vision.[46]

Although, these nanoparticles don't fall under molecular TTA-UC category, the approach gives interesting insight of using NIR to Vis molecular TTA-UC by developing NIR image vision contact lenses, functioning at low NIR excitation intensities. Moreover, further research is needed to synthesize heavy atom free triplet sensitizers or sensitizer free NIR to Vis TTA-UC annihilators to minimize the toxicity issues for *in vivo* applications beyond proof of concept.

7. Summary, challenges and future directions

Since, Baluschev's report in 2007,[24] NIR to Vis TTA-UC systems have evolved beyond deoxygenated organic solvents to oxygen stable solid state and aqueous environments to realize practical feasibility. The evolution is accompanied by the introduction of new ISC route (direct S_0-to-T_1 absorption),[6,23,38–40] inorganic–organic hybrid systems,[12,15,34–36,42] new TET route (sensitizer-transmitter-annihilator,[34–36] sensitizer–annihilator-emitter[12,42]), NIR harvesting beyond 950 nm,[15,34,37,41] thermally activated delayed phosphorescent sensitizer,[6] photostable annihilator,[28,29,32] σ-π

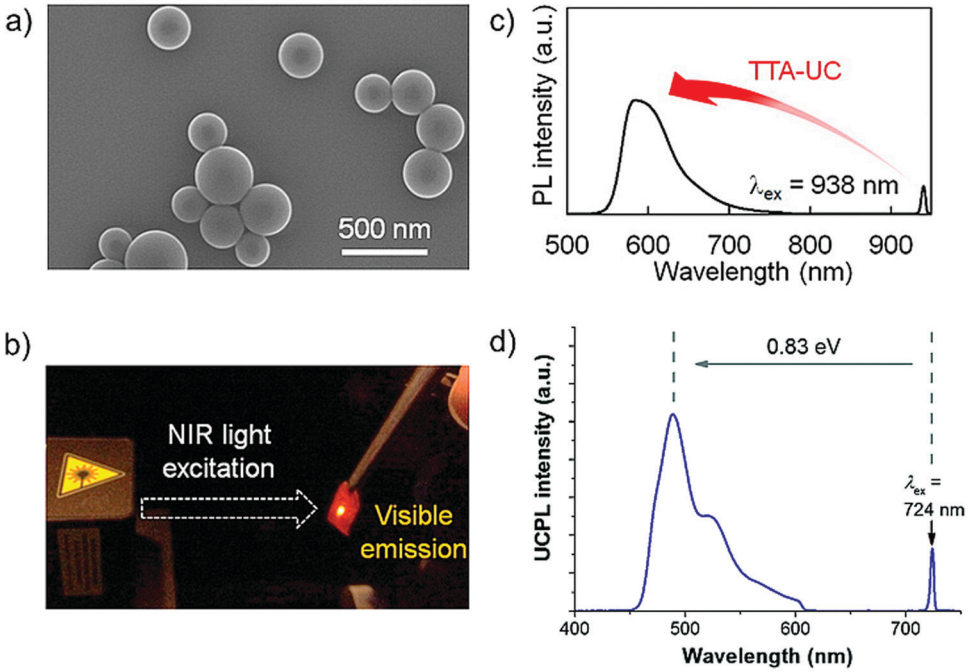

Fig. 27 (a) SEM image of the osmium complex(sensitizer)-doped rubrene (annihilator) nanoparticles. (b) Photograph of upconverted yellow emission of osmium complex-rubrene in PVA film in air under 938 nm NIR excitation. (c) In-air upconverted emission spectrum of the osmium complex-doped rubrene NPs dispersed in PVA film (λ_{ex} = 938 nm, 780 nm short pass filter). (d) Photoluminescence spectra of $Os(bptpy)_2^{2+}$-TTBP in the PVA film (λ_{ex} = 724 nm, 610 nm short pass filter, λ_{ex} = 43 W cm^{-2}).[38,39] Reproduced with permission from ref. 38 and 39. Copyrights 2016, American Chemical Society and 2017 The Royal Society of Chemistry.

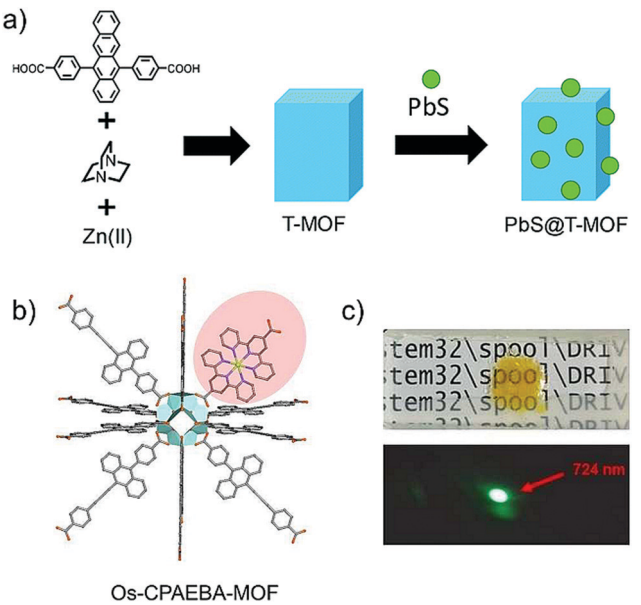

Fig. 28 (a) Schematic illustration of the PbS@T-MOF for NIR-to-visible TTA-UC. (b) Schematic diagram of Os-sensitizer incorporated into CPAEBA-MOF annihilator framework and (c) photograph of Os-CPAEBA-MOF@TNB under white light (above) and 724 nm laser light excitation. Reproduced with permission from ref. 22 and 23. Copyrights 2018, The Royal Society of Chemistry and 2020, Wiley-VCH Verlag GmbH & Co. KGaA, Weinheim.

conjugated annihilator,[40] NIR to Vis TTA-UC MOF's,[22,23] hydrogel,[6] liquid crystals,[20] nanoparticles,[5,38,39] oxygen stable fabrication techniques,[5,6,23,26,38,39] spectral upconversion range 1140 nm to 415 nm[15,37,40] and practical applications in solar cells,[1,2] photocatalysis,[4] bioimaging[5] and optogenetics.[6]

The molecular TTA-UC is considered advantageous over TPA and rare earth metal doped UC nanocrystals based on the potential to achieve high UC quantum yield at low threshold excitation intensities. Indeed, the reported NIR to Vis TTA-UC systems have certainly proved it correct. The maximum UC quantum yield obtained till date for NIR to Vis TTA-UC system is $\Phi_{UC} \sim 5.5\%$ in deoxygenated organic solvent[18,40] and Φ_{UC} = 3.5 ± 0.5% in a degassed solid device.[12] At the excitation intensity front, the lowest I_{th} = 3.2 mW cm^{-2} is reported for the inorganic core–shell sensitizer–transmitter–annihilator system in deoxygenated organic solvent[36] and 240 mW cm^{-2} for S_0-to-T_1 sensitized degassed cyclophane annihilator solid.[20] However, realizing such high efficiencies and low I_{th} in aerated environments is still a big challenge. Additionally, aggregation induced fluorescence quenching of chromophores, further lowers the efficiencies in the solid state. Considering the low energy and deep penetrative nature of NIR light, the low I_{th} and high Φ_{UC} may not be the essential requirements for biological applications, but oxygen protection of triplets and cytotoxicity are. While the heavy metal-based sensitizers have shown suitability for UC blue light responsive optogenetic and bioimaging application,[5,6] their toxicity still remains an issue for practical *in vivo* experiments. Developing physiological pH stable caged UC nanogels would be an ideal platform for practical utility of these systems. Further, developments in heavy atom free

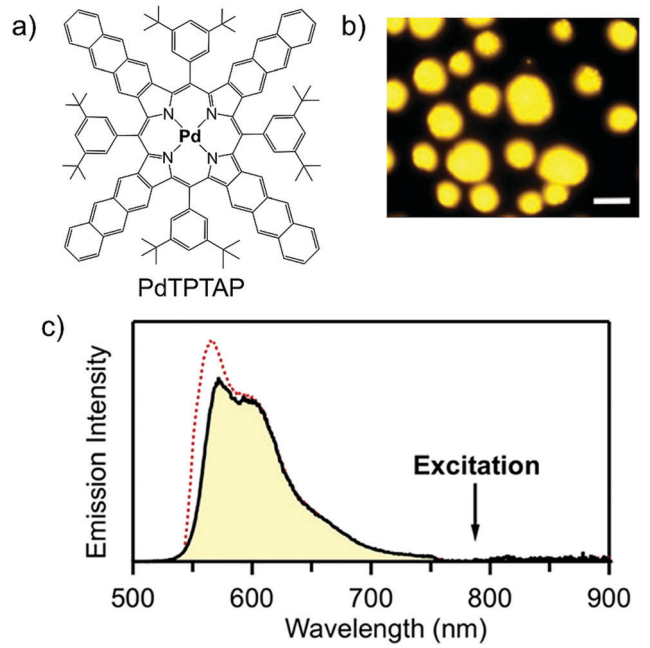

Fig. 29 (a) Molecular structure of the PdTPTAP (sensitizer). (b) UC emission image of microparticles of the binary solid. The scale bars are 50 μm, λ_{ex} = 785 nm. (c) UC emission spectrum of a single microparticle under aerated conditions at the intensity of 7 W cm^{-2} at the sample position (black solid curve filled with yellow, with a 785 nm notch filter) and normal fluorescence from rubrene neat solid excited at 532 nm (red dotted).[43] Reproduced with permission from ref. 43. Copyrights 2019, American Chemical Society.

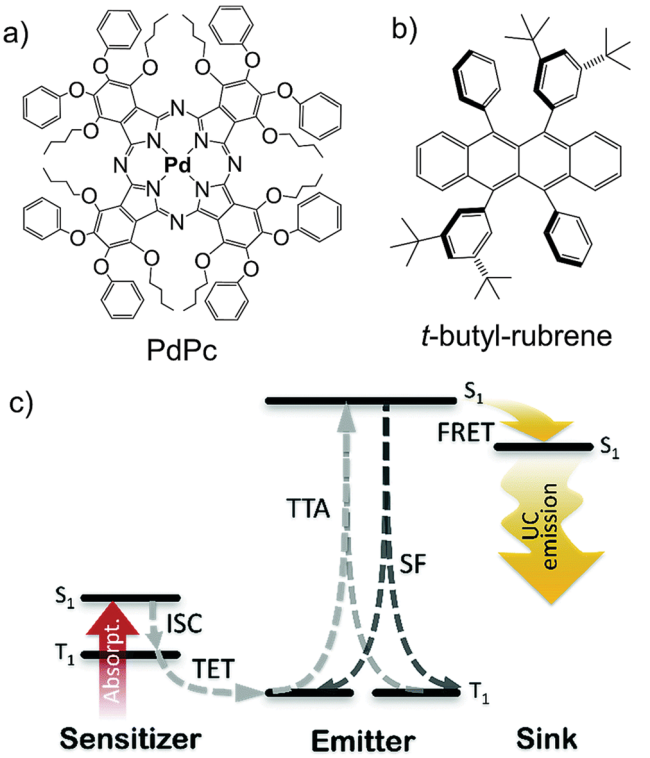

Fig. 30 (a) and (b) Molecular structures of the (a) PdPc (sensitizer), and (b) *t*-butyl-rubrene (annihilator). (c) TTA-UC energy scheme for PdPc-sensitized rubrene (or TBR) systems with DBP as a singlet sink. Here, ISC-intersystem crossing, TET-triplet energy transfer, TTA-triplet–triplet annihilation, SF-singlet fission, FRET-Förster resonant energy transfer. Reproduced with permission from ref. 44. Copyright 2020, The Royal Society of Chemistry.

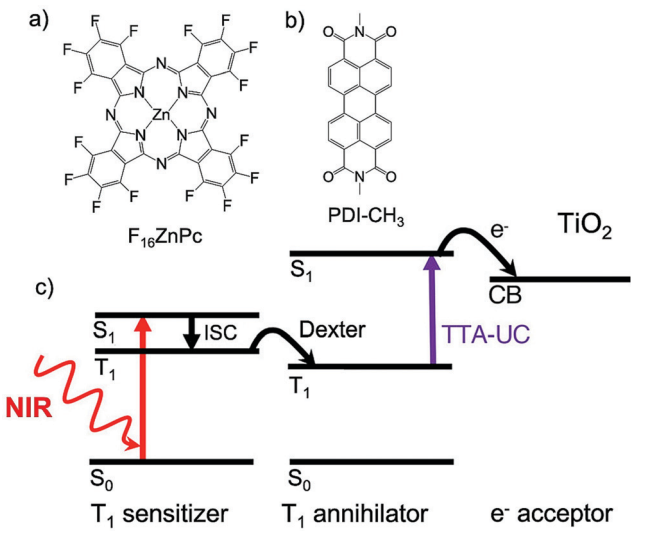

Fig. 31 (a) and (b) Molecular structures of the (a) $F_{16}ZnPc$ (sensitizer), and (b) PDI-CH_3 (annihilator). (c) Schematic of the electron injection into TiO_2 by upconverted singlet excited state of annihilator after triplet sensitization by sensitizer upon NIR light absorption. Reproduced from ref. 45. Copyright 2019, American Chemical Society.

thiosquaraine[47] and BODIPY[15] as TTA-UC sensitizer for showing TTA-UC from >700 to <500 nm, can give suitable solution to develop non-toxic bio-nanovehicles for bio-applications. The squaraine dyes are well known for their biomedical applications due to their low toxicities.[47] Moreover, cutting out the sensitizer's role by developing sensitizer free NIR to Vis TTA-UC with water soluble and cytocompatible dye like fluorescein would provide a promising alternative research platform for bio-applicable NIR to Vis TTA-UC. Besides, optogenetic, photodynamic therapy and bioimaging applications, we think that molecular TTA-UC should be exploited for nocturnal vision using NIR light stimulation[46] by developing NIR to Vis TTA-UC contact lenses. Kimizuka and Yanai's research group (Bharmoria *et al.*)[19] has reported Vis to Vis TTA-UC hydrogels of fibrous protein gelatin which shares phylogeny with collagen present in the cornea of eye. Well, such fibrous proteins can be used to form NIR to Vis TTA-UC lenses by suitable tuning of chromophores. While the commercial contact lenses are made up of silicon hydrogel, their coating with transparent protein fabricated TTA-UC materials can potentially incorporate nocturnal vision in them. Additionally, it is highly desired to have soluble and non-aggregating chromophores in protein solution to materialize such systems. It can be achieved by forming salts of NIR annihilator, while retaining significant fluorescence quantum yields using a facile approach.[19]

The high Φ_{UC} of S_0-to-T_1 sensitized NIR to Vis TTA-UC systems are highly suitable for NIR stimulated photocatalytic synthesis and solution integrated solar cells.[39,40] Further efforts in this direction are desired to realize aerobic photocatalysis employing these systems as dispersed catalytic phase in organogels

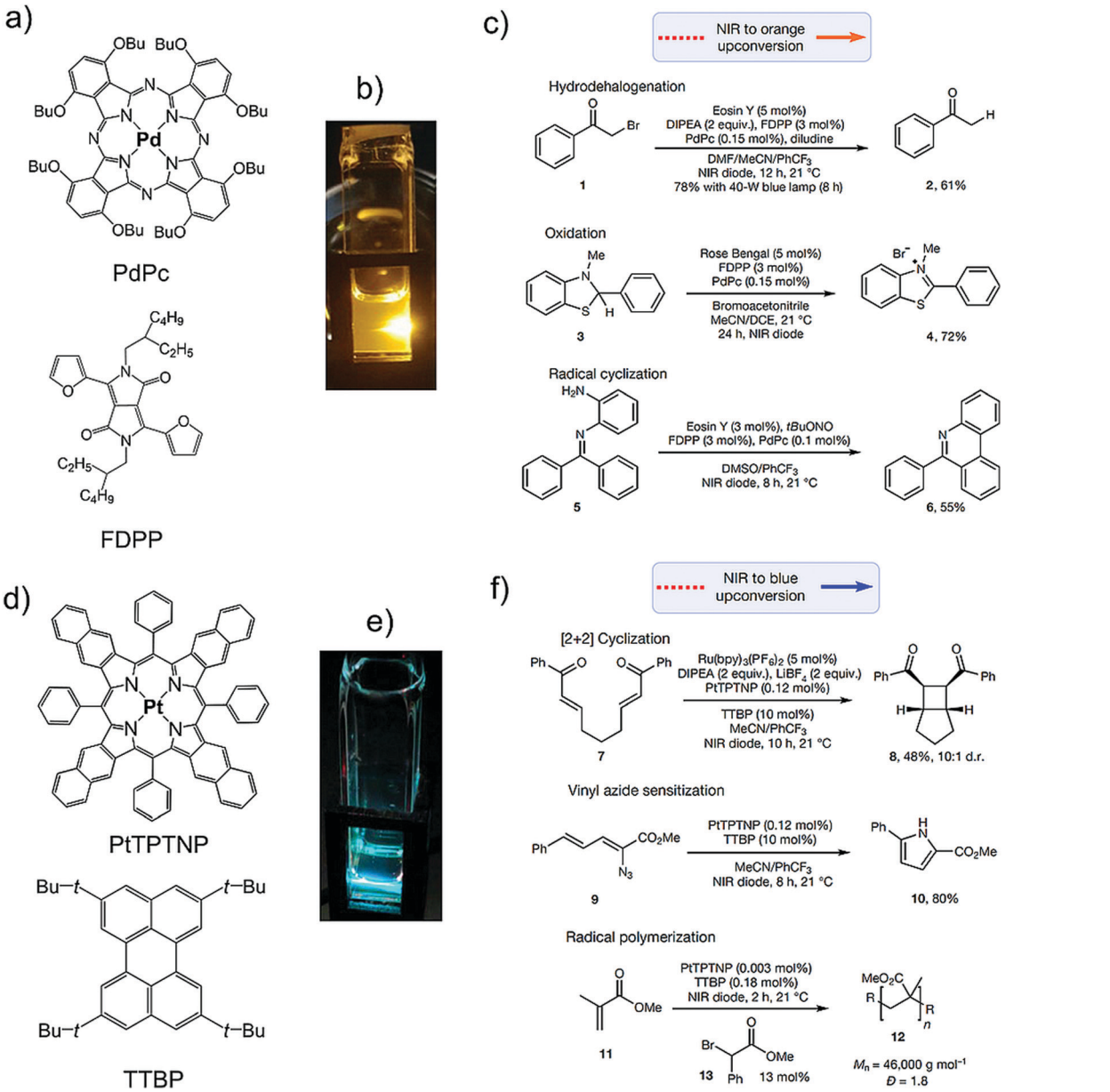

Fig. 32 (a)–(c) NIR to orange TTA-UC catalysed photoreduction. (a) Molecular structure of PdPc (sensitizer) and, FDPP (annihilator). (b) Photograph of NIR to orange TTA-UC. (c) Hydrodehalogenation reaction catalysed by Eosin Y, Amine oxidation catalysed by Rose Bengal, and reductive radical cyclization yielding a phenanthridine product due to the excitation of photocatalyst by orange upconverted photons. (d)–(f) NIR to blue TTA-UC catalyzed photoreduction. (d) Molecular structure of PtTPTNP (sensitizer), and TTBP (annihilator). (e) Photograph of NIR to blue TTA-UC. (f) Intramolecular [2+2] cyclization, pyrrole formation *via* vinyl azide reduction and polymerization of methylmethacrylate upon photoexcitation with blue upconverted photon. Reproduced with permission from ref. 4. Copyrights 2019, Springer Nature Limited.

and aerobic solid-state NIR to Vis TTA-UC for solar cell integration. In the solid-state NIR to Vis TTA-UC, the major challenge is the aggregation induced fluorescence quenching of the chromophores, additionally supported by secondary quenching pathways like singlet fission. The metal porphyrins have natural tendency of aggregation due to their symmetrical nature even in organic solvents, whereas the nanocrystals sensitizers have challenges with the light absorbing in the upconverted region. Although, the introduction of collector, has improved UC quantum yield in such systems, it is still very low due to issues related to the annihilator (rubrene). These challenges include, photo-degradation in aerated conditions, aggregation induced quenching in the solid state and singlet fission upon upconversion. Even after exhibiting such shortcomings, rubrene is the most used annihilator in NIR to Vis TTA-UC, probably due to the suitable overlap of its electronic state with the newly developed NIR sensitizers. Therefore, in the NIR to Vis TTA-UC research, rubrene is "can't keep can't let" kind of a property. Nevertheless, the photostable variants of rubrene have also been reported by replacing the side phenyl rings with thiophene or furan,[48] which

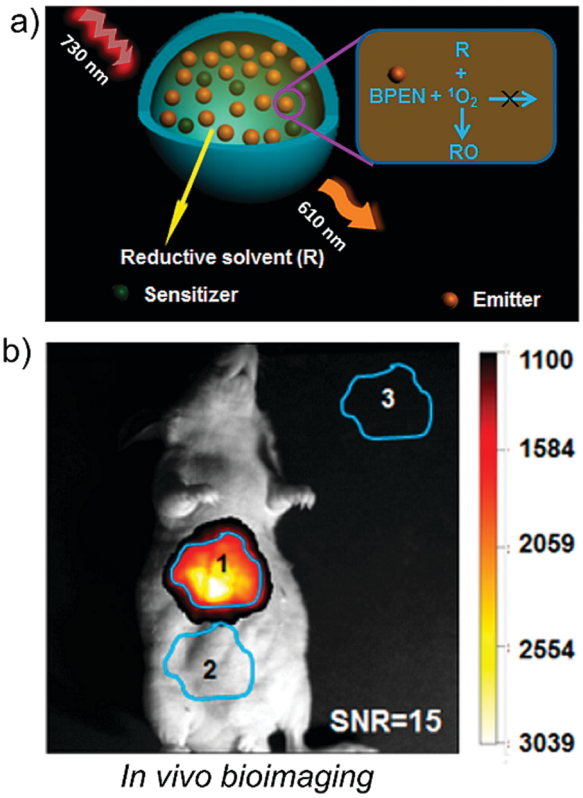

Fig. 33 (a) Schematic of TTA-UC emission by NIR to Vis upconversion nanoparticles. (b) Photograph of *in vivo* TTA-UC emission by mouse body upon 730 nm laser excitation by injected nanoparticles. Reproduced with permission from ref. 5. Copyright 2018, American Chemical Society.

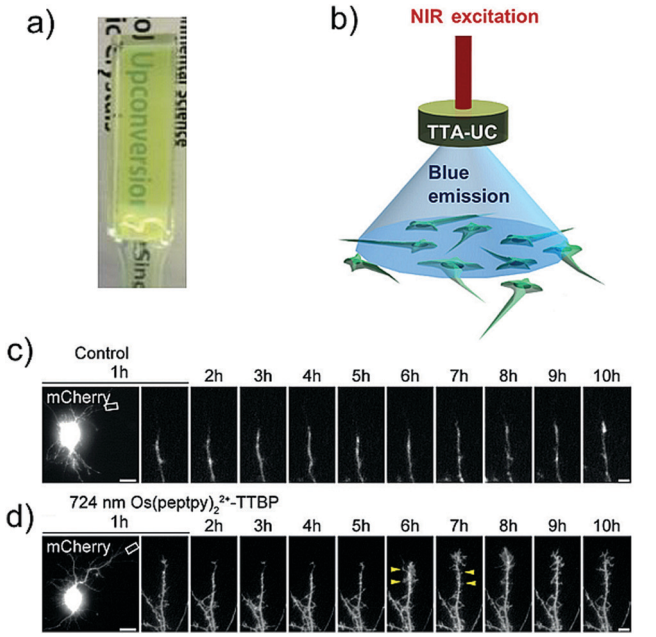

Fig. 34 (a) Photograph of NIR to Vis TTA-UC hydrogel comprising Os(peptpy)$_2^{2+}$ (sensitizer), TTBP (annihilator) and Pluronic f127 as hydrogelator. (b) A schematic representation of NIR optogenetics based on TTA-UC hydrogels after continuous-wave irradiation with NIR laser at 724 nm. (c) and (d) Time-lapse imaging of hippocampal neurons. Arrowheads indicate the formation of dendritic-spine-like structures indicating optogenetic behavior upon exposure to upconverted blue light. Scale bars: 20 mm (left column) and 5 mm (others). Reproduced with permission from ref. 6. Copyright 2019, Wiley-VCH Verlag GmbH & Co. KGaA, Weinheim.

either scavenges the oxygen or limit its interference either sterically or electronically due to the altered HOMO–LUMO energy levels. Besides photostability, these compounds also show aggregation induced emission enhancement, therefore making them suitable for solid state TTA-UC upon integration with suitable NIR sensitizer. Therefore, it is desired to think beyond the conventional approach of tuning HOMO–LUMO energy levels by extending or limiting the π–π conjugation and alternative approaches like, the introduction of new functional group for σ–π conjugation[40] and aromaticity reversal of excited state for enhanced ISC[47] must be explored to design non-toxic and aggregation enhanced luminescent chromophores for efficient and long-range energy upconversion. Another important factor affecting the UC quantum yield is *f* factor, which defines the probability of forming excited singlet state post TTA. Since it competes with quintet and triplet channels, suitable molecular engineering of annihilators is sought to avoid the loss of triplet photons *via* quintet and triplet channel to increase *f* factor and ultimately the Φ_{UC}.[18,44]

Other than chromophore design, fabrication technique is an essential issue to be fixed for an efficient solid state NIR to Vis TTA-UC. Approaches used till date includes dye nanoparticles dispersed synthetic polymers films, chromophore crystals/liquid crystals and polymer dispersed with MOF (degassed or oxygen stable). For example, polyvinyl alcohol (PVA) and polystyrene are polymers used as dispersion medium as part of oxygen protection strategy for NIR to Vis TTA-UC. Although, these systems do provide protection against oxygen, chromophore aggregation resulting in triplet trap site comes in as secondary issue. Other synthetic polymers used for triplet protection against oxygen in solid state include poly-acrylate elastomers, poly-methyl methacrylate, (for Vis to Vis TTA-UC), however ending up with similar fate. Besides these, bio-inspired strategy of oil loaded cellulose nanofiber film, mimicking leaf, both for efficient chromophore dispersion and oxygen protection is also reported.[8] However, oxygen protection is achieved by applying multiple layers of cellulose nanofibers due to oxygen permeation through the single layer. Well, one common feature of synthetic polymers and cellulose is their homopolymer nature, which provides only small hydrophobic zones for molecular dispersion leading to chromophore aggregation. The heteropolymers like, structural proteins can give suitable alternative here due to their differentially polar nature. The protein-lipid films are well known for food packaging application on account of very low oxygen permeation and high thermodynamic stability.[49] Recently protein gelatin has been reported to protect the photochemical degradation and photobleaching of fluorescent protein *R*-phycoerythrin[49] and therefore can be extended to photon upconversion by molecular dispersion of ionic chromophores.

The reabsorption issue of inorganic quantum dot sensitizer in TTA-UC can be mitigated by developing new layering

techniques by controlling the thickness and concentration of quantum dots. Although, the extended π-aromatic chromophore does create aggregation issues, transforming them to supramolecular dendrimers give advantage in terms of restricting triplet energy loss due to annihilator diffusion.[7] Doping the amorphous films of these supramolecular networks with suitable NIR sensitizer, can overturn the inherent triplet energy losses due to diffusion. Further, extension of such supramolecular chromophores to liquid crystalline structure by side chain functionalization with polymers[50] may lead to the next generation inbuilt directed emissive[21] and oxygen resistant NIR to Vis TTA-UC, which our research group is committed to achieving.

Conflicts of interest

There are no conflicts to declare.

Acknowledgements

Pankaj Bharmoria acknowledges Marie Skłodowska-Curie Actions – European Commission post-doctoral grant (NIRLAMS, Grant agreement ID: 844972) for research funding. Hakan Bildirir and Kasper Moth-Poulsen acknowledges funding from the Swedish Energy Agency, the Swedish Research Agency FORMAS, the Swedish Strategic Foundation and the K & A Wallenberg foundation.

References

1 T. F. Schulze, J. Czolk, Y.-Y. Cheng, B. Fückel, R. W. MacQueen, T. Khoury, M. J. Crossley, B. Stannowski, K. Lips, U. Lemmer, A. Colsmann and T. W. Schmidt, *J. Phys. Chem. C*, 2012, **116**, 22794–22801.
2 A. Nattestad, Y. Y. Cheng, R. W. MacQueen, T. F. Schulze, F. W. Thompson, A. J. Mozer, B. Fückel, T. Khoury, M. J. Crossley, K. Lips, G. G. Wallace and T. W. Schmidt, *J. Phys. Chem. Lett.*, 2013, **4**, 2073–2078.
3 V. Gray, D. Dzebo, M. Abrahamsson, B. Albinsson and K. Moth-Poulsen, *Phys. Chem. Chem. Phys.*, 2014, **16**, 10345–10352.
4 B. D. Ravetz, A. B. Pun, E. M. Churchill, D. N. Congreve, T. Rovis and L. M. Campos, *Nature*, 2019, **565**, 343–346.
5 Q. Liu, M. Xu, T. Yang, B. Tian, X. Zhang and F. Li, *ACS Appl. Mater. Interfaces*, 2018, **10**, 9883–9888.
6 Y. Sasaki, M. Oshikawa, P. Bharmoria, H. Kouno, A. Hayashi-Takagi, M. Sato, I. Ajioka, N. Yanai and N. Kimizuka, *Angew. Chem., Int. Ed.*, 2019, **58**, 17827–17833.
7 V. Gray, K. Moth-Poulsen, B. Albinsson and M. Abrahamsson, *Coord. Chem. Rev.*, 2018, **362**, 54–71.
8 M. A. Filatov, S. Baluschev and K. Landfester, *Chem. Soc. Rev.*, 2016, **45**, 4668–4689.
9 C. A. Parker and C. G. Hatchard, *Proc. R. Soc. London, Ser. A*, 1962, 386–387.
10 P. E. Keivanidis, S. Baluschev, T. Miteva, G. Nelles, U. Scherf, A. Yasuda and G. Wegner, *Adv. Mater.*, 2003, **15**, 2095–2098.
11 S. Baluschev, T. Miteva, V. Yakutkin, G. Nelles, A. Yasuda and G. Wegner, *Phys. Rev. Lett.*, 2006, **97**(143903), 1–3.
12 L. Nienhaus, M. Wu, N. Geva, J. J. Shepherd, M. W. B. Wilson, V. Bulović, T. V. Voorhis, M. A. Baldo and M. G. Bawendi, *ACS Nano*, 2017, **11**, 7848–7857.
13 N. Yanai and N. Kimizuka, *Acc. Chem. Res.*, 2017, **50**, 2487–2495.
14 N. Kimizuka, N. Yanai and M. Morikawa, *Langmuir*, 2016, **32**, 12304–12322.
15 N. Nishimura, J. R. Allardice, J. Xiao, Q. Gu, V. Gray and A. Rao, *Chem. Sci.*, 2019, **10**, 4750–4760.
16 L. Lyu, H. Cheong, X. Ai, W. Zhang, J. Li, H. H. Yang, J. Lin and B. Xing, *NPG Asia Mater.*, 2018, **10**, 685–702.
17 Y. Zhou, F. N. Castellano, T. W. Schmidt and K. Hanson, *ACS Energy Lett.*, 2020, **5**, 2322–2326.
18 E. Radiunas, S. Raišys, S. Juršenas, A. Jozeliūnaite, T. Javorskis, U. Šinkevičiūte, E. Orentas and K. Kazlauskas, *J. Mater. Chem. C*, 2020, **8**, 5525–5534.
19 P. Bharmoria, S. Hisamitsu, H. Nagatomi, T. Ogawa, M. Morikawa, N. Yanai and N. Kimizuka, *J. Am. Chem. Soc.*, 2018, **34**, 10848–10855.
20 K. Mase, Y. Sasaki, Y. Sagara, N. Tamaoki, C. Weder, N. Yanai and N. Kimizuka, *Angew. Chem., Int. Ed.*, 2018, **57**, 2806–2810.
21 K. Börjesson, P. Rudquist, V. Gray and K. Moth-Poulsen, *Nat. Commun.*, 2016, **7**(12689), 1–8.
22 S. Amemori, R. K. Gupta, M. L. Böhm, J. Xiao, U. Huynh, T. Oyama, K. Kaneko, A. Rao, N. Yanai and N. Kimizuka, *Dalton Trans.*, 2018, **47**, 8590–8594.
23 B. Joarder, A. Mallick, Y. Sasaki, M. Kinoshita, R. Haruki, Y. Kawashima, N. Yanai and N. Kimizuka, *ChemNanoMat*, 2020, **6**, 1–5.
24 S. Baluschev, V. Yakutkin, T. Miteva, Y. Avlasevich, S. Chernov, S. Aleshchenkov, G. Nelles, A. Cheprakov, A. Yasuda, K. Müllen and G. Wegner, *Angew. Chem., Int. Ed.*, 2007, **46**, 7693–7696.
25 S. Baluschev, V. Yakutkin, T. Miteva, G. Wegner, T. Roberts, G. Nelles, A. Yasuda, S. Chernov, S. Aleshchenkov and A. Cheprakov, *New J. Phys.*, 2008, **10**, 013007.
26 T. N. Singh-Rachford and F. N. Castellano, *J. Phys. Chem. A*, 2008, **112**, 3550–3556.
27 V. Yakutkin, S. Aleshchenkov, S. Chernov, T. Miteva, G. Nelles, A. Cheprakov and S. Baluschev, *Chem. – Eur. J.*, 2008, **14**, 9846–9850.
28 T. N. Singh-Rachford, A. Nayak, M. L. Muro-Small, S. Goeb, M. J. Therien and F. N. Castellano, *J. Am. Chem. Soc.*, 2010, **132**, 14203–14211.
29 B. Fückel, D. A. Roberts, Y. Y. Cheng, R. G. C. R. Clady, R. B. Piper, N. J. Ekins-Daukes, M. J. Crossley and T. W. Schmidt, *J. Phys. Chem. Lett.*, 2011, **2**, 966–971.
30 F. Deng, J. R. Sommer, M. Myahkostupov, K. S. Schanze and F. N. Castellano, *Chem. Commun.*, 2013, **49**, 7406–7408.
31 Y. Liu, W. Wu, J. Zhao, X. Zhang and H. Guo, *Dalton Trans.*, 2011, **40**, 9085–9089.

32 F. Deng, W. Sunb and F. N. Castellano, *Photochem. Photobiol. Sci.*, 2014, **13**, 813–819.
33 S. Amemori, N. Yanai and N. Kimizuka, *Phys. Chem. Chem. Phys.*, 2015, **17**, 22557–22560.
34 Z. Huang, X. Li, M. Mahboub, K. M. Hanson, V. M. Nichols, H. Le, M. L. Tang and C. J. Bardeen, *Nano Lett.*, 2015, **15**, 5552–5557.
35 Z. Huang, D. E. Simpson, M. Mahboub, X. Lia and M. L. Tang, *Chem. Sci.*, 2016, **7**, 4101–4104.
36 M. Mahboub, Z. Huang and M. L. Tang, *Nano Lett.*, 2016, **16**, 7169–7175.
37 E. M. Gholizadeh, S. K. K. Prasad, Z. L. Teh, T. Ishwara, S. Norman, A. J. Petty II, J. H. Cole, S. Cheong, R. D. Tilley, J. E. Anthony, S. Huang and T. W. Schmidt, *Nat. Photonics*, 2020, **14**, 585–590.
38 S. Amemori, Y. Sasaki, N. Yanai and N. Kimizuka, *J. Am. Chem. Soc.*, 2016, **138**, 8702–8705.
39 Y. Sasaki, S. Amemori, H. Kouno, N. Yanai and N. Kimizuka, *J. Mater. Chem. C*, 2017, **5**, 5063–5067.
40 R. Haruki, Y. Sasaki, K. Masutani, N. Yanai and N. Kimizuka, *Chem. Commun.*, 2020, **56**, 7017–7020.
41 N. Kiseleva, P. Nazari, C. Dee, D. Busko, B. S. Richards, M. Seitz, I. A. Howard and A. Turshatov, *J. Phys. Chem. Lett.*, 2020, **11**, 2477–2481.
42 M. Wu, D. N. Congreve, M. W. B. Wilson, J. Jean, N. Geva, M. Welborn, T. V. Voorhis, V. Bulović, M. G. Bawendi and M. A. Baldo, *Nat. Photonics*, 2016, **10**, 31–34.
43 A. Abulikemu, Y. Sakagami, C. Heck, K. Kamada, H. Sotome, H. Miyasaka, D. Kuzuhara and H. Yamada, *ACS Appl. Mater. Interfaces*, 2019, **11**, 20812–20819.
44 E. Radiunas, M. Dapkevičius, S. Raišys, S. Juršenas, A. Jozeliūnaite, T. Javorskis, U. Šinkevičiūte, E. Orentas and K. Kazlauskas, *Phys. Chem. Chem. Phys.*, 2020, **22**, 7392–7403.
45 K. M. Felter, M. C. Fravventura, E. Koster, R. D. Abellon, T. J. Savenije and F. C. Grozema, *ACS Energy Lett.*, 2020, **5**, 124–129.
46 Y. Ma, J. Bao, Y. Zhang, Y. Zhao, G. Han and T. Xue, *Cell*, 2019, **177**, 243–255.
47 S. R. Pristash, K. L. Corp, E. J. Rabe and C. W. Schlenker, *ACS Appl. Energy Mater.*, 2020, **3**, 19–28.
48 M. Mamada, H. Katagiri, T. Sakanoue and S. Tokito, *Cryst. Growth Des.*, 2015, **15**(1), 442–448.
49 P. Bharmoria, S. F. H. Correia, M. Martins, M. A. Hernández-Rodríguez, S. P. M. Ventura, R. A. S. Ferreira, L. D. Carlos and J. A. P. Coutinho, *J. Phys. Chem. Lett.*, 2020, **11**, 6249–6255.
50 T. Kato, H. Kihara, S. Ujiie, T. Uryu and J. M. J. Fréchet, *Macromolecules*, 1996, **29**, 8734–8739.

